The Astrophysical Journal, 758:101 (18pp), 2012 October 20 doi:10.1088/0004-637X/758/2/101

THE PAIR BEAM PRODUCTION SPECTRUM FROM PHOTON–PHOTON ANNIHILATION IN COSMIC VOIDS

R. Schlickeiser[1,2], A. Elyiv[3,4], D. Ibscher[1], and F. Miniati[5]
[1] Institut für Theoretische Physik, Lehrstuhl IV: Weltraum- und Astrophysik, Ruhr-Universität Bochum, D-44780 Bochum, Germany; rsch@tp4.rub.de, ibscher@tp4.rub.de
[2] Research Department Plasmas with Complex Interactions, Ruhr-Universität Bochum, D-44780 Bochum, Germany
[3] Institut d'Astrophysique et de Géophysique, Université de Liège, B-4000 Liège, Belgium; elyiv@astro.ulg.ac.be
[4] Main Astronomical Observatory, Academy of Sciences of Ukraine, 27 Akademika Zabolotnoho St., 03680 Kyiv, Ukraine
[5] Physics Department, Wolfgang-Pauli-Strasse 27, ETH-Zürich, CH-8093 Zürich, Switzerland; fm@phys.ethz.ch
Received 2012 May 27; accepted 2012 August 26; published 2012 October 5

ABSTRACT

Highly beamed relativistic $e^{\pm}$-pair energy distributions result in double photon collisions of the beamed gamma rays from TeV blazars at cosmological distances with the isotropically distributed extragalactic background light (EBL) in the intergalactic medium. The typical energies $k_0 \simeq 10^{-7}$ in units of $m_e c^2$ of the EBL are more than 10 orders of magnitude smaller than the observed gamma-ray energies $k_1 \geqslant 10^7$. Using the limit $k_0 \ll k_1$, we demonstrate that the angular distribution of the generated pairs in the lab frame is highly beamed in the direction of the initial gamma-ray photons. For the astrophysically important case of power-law distributions of the emitted gamma-ray beam up to the maximum energy M interacting with Wien-type $N(k_0) \propto k_0^q \exp(-k_0/\Theta)$ soft photon distributions with total number density N_0, we calculate analytical approximations for the electron production spectrum. For distant objects with luminosity distances $d_L \gg r_0 = (\sigma_T N_0)^{-1} = 0.49 N_0^{-1}$ Mpc (with Thomson cross section σ_T), the implied large values of the optical depth $\tau_0 = d_L/r_0$ indicate that the electron production spectra differ at energies inside and outside the interval $[(\Theta \ln \tau_0)^{-1}, \tau_0/\Theta]$, given the maximum gamma-ray energy $M \gg \Theta^{-1}$. In the case $M \gg \Theta^{-1}$, the production spectrum is strongly peaked near $E \simeq \Theta^{-1}$, being exponentially reduced at small energies and decreasing with the steep power law $\propto E^{-1-p}$ up to the maximum energy $E = M - (1/2)$.

Key words: cosmic rays – diffuse radiation – gamma rays: general – radiation mechanisms: non-thermal – relativistic processes

1. INTRODUCTION

Intergalactic space is transparent to radiation in most of the electromagnetic spectrum. However, gamma rays above GeV energies cannot travel cosmological distances (Aharonian et al. 1994; Neronov & Vovk 2010) as they are converted into electron–positron pairs, $e^{\pm}$, by way of photon–photon interactions with the extragalactic background light (EBL). The mean free path for a gamma-ray photon with energy E_γ is roughly $l_{\gamma\gamma} \sim 80(E_\gamma/10\,\mathrm{TeV})^{-1}(1+z)^{-\xi}$ Mpc, with $\xi = 4.5$ for redshifts $z \leqslant 1$, $\xi = 0$ otherwise (Kneiske et al. 2004; Franceschini et al. 2008; Neronov & Semikoz 2009), and the exact value depending on the uncertain details of the EBL. This photon absorption process produces a cutoff in the multi-TeV part of the radiation spectrum of distant blazars, a subclass of active galactic nuclei with high-energy photon emission from relativistic jet emission preferentially aligned to the observer's line of sight. Figure 1 depicts the physical situation.

Currently, about 30 blazars with strong TeV photon emission have been detected by the new generation of air Cherenkov TeV γ-ray telescopes such as H.E.S.S., MAGIC, and VERITAS (Hinton & Hofmann 2009). The most distant ones are 3C66A at redshift $z = 0.444$ and 1ES 0414+009 (Abramowski et al. 2012) at redshift $z = 0.287$. Any blazars more distant than $z = 0.16$ produce energetic pair beams.

The study of blazars at TeV energies provides important constraints on the properties of the EBL (Aharonian et al. 2006); it can also be used to probe magnetic fields in cosmic voids (Neronov & Vovk 2010). Each particle of the initially gamma ray produced $e^{\pm}$ pair beam carries about half the energy of the parent gamma ray. Those pairs with typical Lorentz factors $\gamma = 10^6 \gamma_6$ are expected to inverse Compton (IC) scatter on the cosmic microwave background (CMB) radiation, on a typical length scale $l_{\mathrm{IC}} \sim 0.75 \gamma_6^{-1}(1+z)^{-4}$ Mpc, thus producing gamma rays with energy of the order of 100 GeV. Given the still relatively short IC interaction length l_{IC}, both pair production and IC emission occur primarily in cosmic voids, which fill most of the cosmic volume. The IC-scattered gamma rays then are still energetic enough for further pair production interactions, which give rise to a full electromagnetic cascade. Knowing the initial blazar's photon spectrum and the EBL, the full electromagnetic cascade can be computed. The total multi-GeV flux, from both the intrinsic and cascade components, contributes to the point-source emission, provided no magnetic field deflects the $e^{\pm}$ pairs on the distance ℓ_{IC}.

However, the pair beam is subject to two-stream-like instabilities of both electrostatic and electromagnetic nature. It has been argued that in this case the cascade would not contribute to the multi-GeV flux and the pair beam energy would be transferred to the intergalactic medium (IGM) with important consequences for its thermal history (Broderick et al. 2012). Another possibility is that the instability saturates early on due to nonlinear effects, leaving a marked footprint on the energy distribution of the beam particles. This has important observational consequences for the cascade (Schlickeiser et al. 2012).

In the first part of this study, we investigate in detail the relaxation of charged pair beams generated by beamed blazar TeV gamma-ray emission in the partially ionized electron–proton IGM. We show that the angular distribution of the generated pairs is highly beamed along the direction of the incoming gamma rays. The analytical form of the energy spectrum of beamed pairs is determined and compared with numerical simulation results. We also demonstrate that the final pair energy distribution is relatively narrow and peaks at $m_e c^2/\Theta$, where

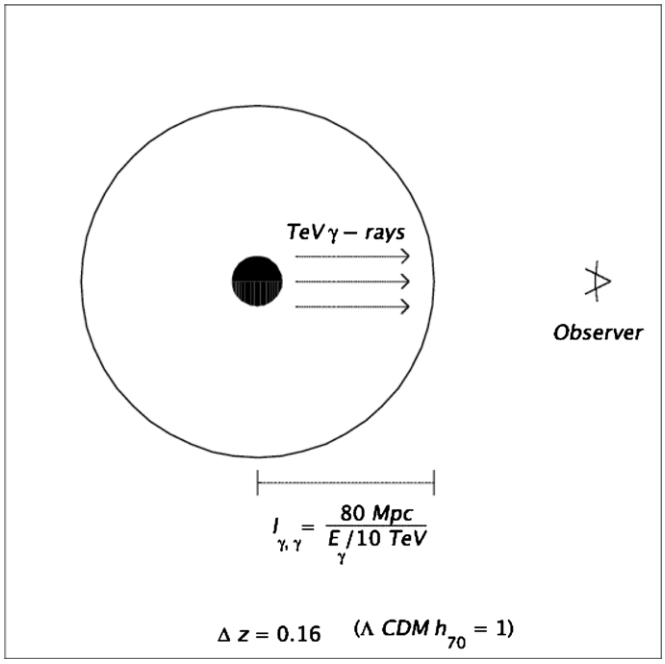

Figure 1. Intergalactic pair beam production: TeV photons from any blazar more distant than $z = 0.16$ produce relativistic pairs by double photon collisions with the EBL soft photons. The mean free path for a gamma-ray photon $l_{\gamma\gamma} \sim 80(E_\gamma/10\,\mathrm{TeV})^{-1}$ Mpc has been converted to a redshift adopting a ΛCDM universe with the Hubble constant $H_0 = 70\,h_{70}$ km s^{-1} Mpc^{-1}.

Θmc^2 with $\Theta \ll 1$ denotes the mean energy of the soft target photons.

Using these and other results from this paper, in the second part of this project (Schlickeiser et al. 2012) we calculate the maximum linear growth rates of the obliquely propagating electrostatic waves and the aperiodic filamentation instability.

The rest of the paper is organized as follows: In Sections 2–4, we derive the injected pair distribution function from the double-photon pair production of blazar gamma radiation with the EBL. The single gamma-ray pair production optical depth is calculated in Section 5. In Sections 6–8, we analytically calculate the electron pair production energy spectrum, starting from the general expression for arbitrary input blazar gamma-ray spectra and arbitrary EBL photon spectra (Section 6), and then specializing to power-law-distributed gamma rays and Wien-type soft photon distributions (Section 7). In Section 8, we provide the pair production spectra in different energy regimes. The results are summarized in Sections 9 and 10.

2. RELATIVISTIC KINEMATICS OF PAIR PRODUCTION BY DOUBLE PHOTON COLLISION

The rest frame of the IGM is chosen as the laboratory (lab) frame. Photon and particle energies and momenta are defined in units of $m_e c^2$ and m_{ec}, respectively. A high-energy ($k_1 \gg 1$) gamma ray with four-momentum $P_1 = k_1(1, \boldsymbol{e}_1)$, where the unit vector $\boldsymbol{e}_1$ defines its direction, interacts with a soft ($k_2 \ll 1$) photon of the EBL with four-momentum $P_2 = k_2(1, \boldsymbol{e}_2)$. The four-momenta of the produced positron and negatron are $P_+ = (E_+, \boldsymbol{p}_+)$ and $P_- = (E_-, \boldsymbol{p}_-)$, respectively, with $E_\pm^2 = p_\pm^2 + 1$.

As usual (Hagedorn 1973) we also introduce the center-of-momentum (CM) frame, defined by

$$k_1^* \boldsymbol{e}_1^* + k_2^* \boldsymbol{e}_2^* = 0. \tag{1}$$

Using the Lorentz invariance of scalar products of four-vectors, we calculate the invariant as

$$s = \frac{1}{4}(P_1 + P_2)^2 = \frac{1}{4}(P_1^* + P_2^*)^2 = \frac{k_1 k_2}{2}(1-\mu) = \frac{1}{4}(k_1^* + k_2^*)^2, \tag{2}$$

with $\mu = \cos\theta = \boldsymbol{e}_1 \cdot \boldsymbol{e}_2$, where θ denotes the angle between the two photon directions in the lab frame. For head-on ($\mu = -1$) collisions, the invariant s attains its maximum value $s_m = k_1 k_2$. The threshold energy for the creation of pairs in the CM frame is $E_{\mathrm{th}}^* = 2$ and requires values of $s \geqslant 1$, providing in the laboratory frame

$$k_1 k_2 \geqslant 1. \tag{3}$$

Pair production then occurs for values of

$$1 \leqslant s \leqslant s_m = k_1 k_2. \tag{4}$$

Energy and momentum conservation of the $\gamma_1 + \gamma_2 \rightarrow e_+ + e_-$ interaction in the CM-frame require

$$k_1^* + k_2^* = E_+^* + E_-^* \tag{5}$$

and $\boldsymbol{p}_+^* + \boldsymbol{p}_-^* = 0$. The last relation provides

$$\boldsymbol{p}_+^* = -\boldsymbol{p}_-^* = \boldsymbol{p}_0^* = p_0^* \boldsymbol{e}_0^*, \tag{6}$$

so that $E_+^* = E_-^* = E_0^*$ are equal. With Equations (1) and (2), condition (5) then becomes

$$E_0^* = \frac{k_1^* + k_2^*}{2} = s^{1/2}, \tag{7}$$

implying $p_0^* = \sqrt{E_0^{*2} - 1} = \sqrt{s-1}$, so that

$$\boldsymbol{p}_+^* = -\boldsymbol{p}_-^* = \boldsymbol{p}_0^* = \sqrt{s-1}\,\boldsymbol{e}_0^*. \tag{8}$$

The CM velocity as seen from the laboratory frame is

$$\boldsymbol{\beta}_{\mathrm{CM}} = \frac{k_1 \boldsymbol{e}_1 + k_2 \boldsymbol{e}_2}{k_1 + k_2}, \tag{9}$$

so that

$$\beta_{\mathrm{CM}}^2 = \frac{k_1^2 + k_2^2 + 2k_1 k_2 \mu}{(k_1 + k_2)^2} = 1 - \frac{2k_1 k_2 (1-\mu)}{(k_1 + k_2)^2} \tag{10}$$

and

$$\gamma_{\mathrm{CM}} = \left(1 - \beta_{\mathrm{CM}}^2\right)^{-1/2} = \left[\frac{(k_1 + k_2)^2}{2k_1 k_2 (1-\mu)}\right]^{1/2}. \tag{11}$$

So far, all relations are exact and no approximations have been made.

Given that the EBL photon energies $k_2 \ll 1$ are very small, the threshold condition (3) requires $k_1 \geqslant k_2^{-1} \gg 1$. We therefore approximate relation (10) by (Bonometto & Rees 1971; Aharonian et al. 1983; Cerutti et al. 2009)

$$\beta_{\mathrm{CM}}^2 \simeq 1 - \frac{2k_1 k_2 (1-\mu)}{k_1^2} = 1 - \frac{4s}{k_1^2}, \tag{12}$$

providing

$$\beta_{\mathrm{CM}} \simeq \beta_C \equiv \sqrt{1 - \frac{4s}{k_1^2}}, \quad \gamma_{\mathrm{CM}} \simeq \gamma_C = \frac{k_1}{2s^{1/2}}$$

and

$$\beta_{\rm CM}\gamma_{\rm CM} \simeq \sqrt{(\gamma_C - 1)(\gamma_C + 1)}, \quad (13)$$

where we used the invariant (2).[6] With the same approximation $k_1 \gg k_2$, Equation (9) provides $\boldsymbol{\beta}_{\rm CM} \parallel \boldsymbol{e}_1$, i.e.,

$$\boldsymbol{\beta}_{\rm CM} \simeq \beta_C \boldsymbol{e}_1 = \sqrt{1 - \frac{4s}{k_1^2}}\boldsymbol{e}_1, \quad (14)$$

so that the CM frame propagates along the same direction as the high-energy gamma ray. This implies that the gamma-ray direction is unchanged $\boldsymbol{e}_1 = \boldsymbol{e}_1^*$ in the two frames of reference.

Finally we have to calculate the pair energies and momentum vectors in the laboratory frame with the appropriate Lorentz transformations of Equations (6) and (7). For the pair energies we obtain

$$\begin{aligned} E_\pm &= \gamma_C[E_0^* \pm \boldsymbol{\beta}_C \cdot \boldsymbol{p}_0^*] \\ &= \frac{k_1}{2s^{1/2}}\left[s^{1/2} \pm \left(1 - \frac{4s}{k_1^2}\right)^{1/2}(s-1)^{1/2}\boldsymbol{e}_1 \cdot \boldsymbol{e}_0^*\right] \\ &= \frac{k_1}{2}[1 \pm F(s,k_1)\mu_e^*] \end{aligned} \quad (15)$$

with

$$F(s,k_1) = \left(\left(1 - \frac{4s}{k_1^2}\right)\left(1 - \frac{1}{s}\right)\right)^{1/2} \quad (16)$$

and $\mu_e^* = \boldsymbol{e}_1 \cdot \boldsymbol{e}_0^* = \boldsymbol{e}_1^* \cdot \boldsymbol{e}_0^*$ denoting the cosine of the angle between the positron and the incoming gamma ray in the CM system. Equation (15) readily yields the relation

$$\mu_e^* = \pm\frac{\frac{2E_\pm}{k_1} - 1}{F(s,k_1)}. \quad (17)$$

Likewise

$$\begin{aligned} \boldsymbol{p}_\pm &= \boldsymbol{p}_\pm^* + \boldsymbol{\beta}_C\gamma_C\left[\tfrac{\gamma_C}{\gamma_C+1}\boldsymbol{\beta}_C \cdot \boldsymbol{p}_\pm^* + E_0^*\right] \\ &= \pm(s-1)^{1/2}\boldsymbol{e}_0^* + \beta_C\gamma_C s^{1/2}\boldsymbol{e}_1\left[1 \pm \tfrac{\beta_C\gamma_C\left(1-\frac{1}{s}\right)^{1/2}}{\gamma_C+1}\boldsymbol{e}_1 \cdot \boldsymbol{e}_0^*\right] \\ &= \pm(s-1)^{1/2}\boldsymbol{e}_0^* + \tfrac{k_1}{2}\left(1 - \tfrac{4s}{k_1^2}\right)^{1/2}\boldsymbol{e}_1\left[1 \pm \tfrac{k_1}{k_1+2s^{1/2}}F(s,k_1)\mu_e^*\right]. \end{aligned} \quad (18)$$

Taking the scalar product of the last equation with $\boldsymbol{e}_1$, we find for the cosine of the angle between the outgoing electrons and the incoming gamma ray $\mu_e = \boldsymbol{e}_1 \cdot \boldsymbol{p}_\pm/p_\pm$ in the laboratory frame

$$\begin{aligned} \mu_e p_\pm &= \pm(s-1)^{1/2}\mu_e^* \\ &\quad + \frac{k_1}{2}\left(1 - \frac{4s}{k_1^2}\right)^{1/2}\left[1 \pm \frac{k_1 F(s,k_1)\mu_e^*}{k_1 + 2s^{1/2}}\right], \end{aligned} \quad (19)$$

where we infer from Equation (15)

$$p_\pm = \sqrt{E_\pm^2 - 1} = \frac{k_1}{2}\left[(1 \pm F(s,k_1)\mu_e^*)^2 - \frac{4}{k_1^2}\right]^{1/2}. \quad (20)$$

[6] As an aside, we note that these approximations give very accurate results—as the more general study, avoiding these assumptions, has demonstrated; see Böttcher & Schlickeiser (1997).

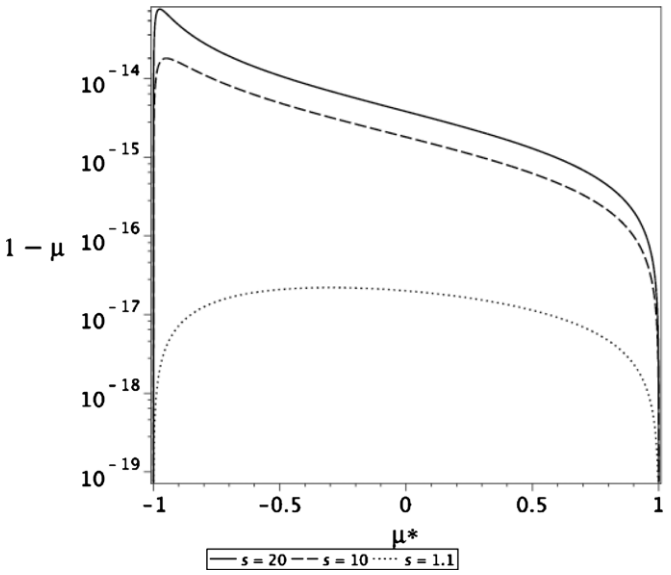

Figure 2. Forward beaming of the generated electrons in the laboratory frame. Shown are the deviations from the forward direction ($\mu = \mu_e = 1$) of electrons in the laboratory frame as a function of the isotropic electron direction in the center-of-momentum frame ($\mu^* = \mu_e^*$) for three values of $s = 1.1$, $s_m/2$, and s_m, where $s_m = k_1k_2 = 20$ denotes the maximum value of the invariant s, corresponding to a monoenergetic gamma-ray beam $k_2 = 10^8$ (51.1 TeV) interacting with a monoenergetic soft photon $k_0 = 2 \times 10^{-7}$ (corresponding 0.1 eV) of EBL.

Combining the last two equations we obtain

$$\begin{aligned} \mu_e = &\left[\frac{1 - \frac{4s}{k_1^2}}{(1 \pm F(s,k_1)\mu_e^*)^2 - \frac{4}{k_1^2}}\right]^{1/2} \\ &\times \left(1 \pm \mu_e^*\left[\frac{k_1 F(s,k_1)}{k_1 + 2s^{1/2}} + 2\sqrt{\frac{s-1}{k_1^2 - 4s}}\right]\right). \end{aligned} \quad (21)$$

3. FORWARD BEAMING OF PAIR-PRODUCED ELECTRONS

Because we cannot distinguish between negatrons and positrons, we infer from Equation (21) that electrons are produced with values of

$$\begin{aligned} \mu_e = &\left[\frac{1 - \frac{4s}{k_1^2}}{(1 + F(s,k_1)\mu_e^*)^2 - \frac{4}{k_1^2}}\right]^{1/2} \\ &\times \left(1 + \mu_e^*\left[\frac{k_1 F(s,k_1)}{k_1 + 2s^{1/2}} + 2\sqrt{\frac{s-1}{k_1^2 - 4s}}\right]\right) \end{aligned} \quad (22)$$

for $\mu_e^* \in [-1, 1]$. In Figure 2, we calculate the resulting electron angular distribution in the laboratory frame $\mu_e(\mu_e^*)$ for the three values of $s = 1.1$, $s_m/2$, and s_m, where $s_m = k_1k_2$ denotes the maximum value of the invariant s. We adopt a 50 TeV gamma ray ($k_1 = 10^8$) and a 0.1 eV EBL photon ($k_2 = 2 \times 10^{-7}$) so that $s_m = 20$. In all three cases, the resulting electron angular distribution is highly beamed in the forward ($\mu_e = 1$) direction. For electrons produced at threshold ($s = 1$), we note $F(1, k_1) = 0$, so that Equation (22) reduces to $\mu_e = 1$ for all values of μ_e^*. With $1 - \mu_e \simeq \theta_e^2/2$ for small angles and $1 - \mu_e \leqslant 10^{-13}$, from Figure 2 we find that the angular spread of the initially generated electrons is less than 5×10^{-7} rad with respect to the incoming gamma-ray direction.

4. ELECTRON ENERGY SPECTRUM

According to Equation (7), the energy of the produced electrons in the CM frame is $E^* = s^{1/2} = (1-\beta^{*2})^{-1/2}$, so that the electron velocity is

$$\beta^* = \left[1 - \frac{1}{s}\right]^{1/2}. \tag{23}$$

Following earlier work (Bonometto & Rees 1971; Cerutti et al. 2009), the probability of a single gamma ray of energy k_1 being absorbed between the path length l and $l+dl$, yielding an electron of energy between E and $E+dE$ and a positron of energy between $k_1 - E - dE$ and $k_1 - E$, in the lab frame is given by

$$\begin{aligned} g(E) &= \int_0^{2\pi} d\phi \int_{-1}^{1} d\mu \int_0^{\infty} dk_2 \, \frac{dn}{dk_2 d\phi d\mu}(1-\mu)\frac{d\sigma_{\gamma\gamma}}{dE} \\ &= \frac{4}{k_1^2}\int_0^{2\pi} d\phi \int_0^{\infty} \frac{dk_2}{k_2^2} \\ &\quad \times \int_0^{k_1 k_2} ds\, s H[s-1] \frac{dn}{dk_2 d\phi d\mu(s)} \frac{d\sigma_{\gamma\gamma}}{dE}, \end{aligned} \tag{24}$$

where we replaced the μ-integration according to Equation (2) with the corresponding s-integration and where the step function $H[s-1]$ accounts for the threshold condition (4). The differential cross section is given by

$$\frac{d\sigma_{\gamma\gamma}}{dE} = \frac{d(\beta^*\mu_e^*)}{dE}\frac{d\sigma_{\gamma\gamma}}{d(\beta^*\mu_e^*)} \tag{25}$$

with (Jauch & Rohrlich 1955; Gould & Schreder 1967; Bonometto & Rees 1971)

$$\begin{aligned} \frac{d\sigma_{\gamma\gamma}}{d(\beta^*\mu_e^*)} &= \frac{3\sigma_T}{16}(1-\beta^{*2}) \\ &\quad \times \frac{1-(\beta^*\mu_e^*)^4 + 2(1-\beta^{*2})[\beta^{*2} - (\beta^*\mu_e^*)^2]}{[1-(\beta^*\mu_e^*)^2]^2}, \end{aligned} \tag{26}$$

where $\sigma_T = 6.65 \times 10^{-25}$ cm^2 denotes the Thomson cross section. Equation (15), used in the form

$$E = \frac{k_1}{2}[1 + F(s,k_1)\mu_e^*] \tag{27}$$

with Equation (23), readily provides

$$\begin{aligned} \frac{d(\beta^*\mu_e^*)}{dE} &= \left[1-\frac{1}{s}\right]^{1/2}\frac{d\mu_e^*}{dE} \\ &= \frac{2\left[1-\frac{1}{s}\right]^{1/2}}{k_1 F(k_1,s)} = \frac{2}{k_1\left[1-\frac{4s}{k_1^2}\right]^{1/2}}. \end{aligned} \tag{28}$$

With

$$A = 1 - \frac{2E}{k_1} \tag{29}$$

we find

$$\beta^*\mu_e^* = \frac{\left(\frac{2E}{k_1}-1\right)\left[1-\frac{1}{s}\right]^{1/2}}{F(k_1,s)} = -\frac{A}{\left[1-\frac{4s}{k_1^2}\right]^{1/2}}, \tag{30}$$

so that the probability (24) becomes

$$\begin{aligned} g(E) &= \frac{3\sigma_T}{2k_1^3}\int_0^{2\pi} d\phi \int_{k_1^{-1}}^{\infty}\frac{dk_2}{k_2^2} \\ &\quad \times \int_1^{k_1 k_2} ds\, \frac{dn}{dk_2 d\phi d\mu} M(A,s) \end{aligned} \tag{31}$$

with

$$\begin{aligned} &M(A,s) = \\ &\frac{\left(1-\frac{4s}{k_1^2}\right)^{1/2}}{1-A^2-\frac{4s}{k_1^2}}\left[\frac{2+s}{s} + \frac{A^2}{1-\frac{4s}{k_1^2}} - \frac{2\left(1-\frac{4s}{k_1^2}\right)}{s^2\left[1-A^2-\frac{4s}{k_1^2}\right]}\right]. \end{aligned} \tag{32}$$

According to Equation (27), with $-1 \leqslant \mu_e^* \leqslant 1$, the electron energies are restricted to the range

$$\begin{aligned} &E_- \leqslant E \leqslant E_+ \\ &E_\pm = \frac{k_1}{2}[1 \pm F(s,k_1)], \end{aligned} \tag{33}$$

corresponding with the definition (29)

$$A^2 = \left(1 - \frac{2E}{k_1}\right)^2 \leqslant F^2(s,k_1) = 1 + \frac{4}{k_1^2} - \left(\frac{1}{s} + \frac{4s}{k_1^2}\right). \tag{34}$$

The last equation yields

$$W(k_1,E) \geqslant s + \frac{k_1^2}{4s} \tag{35}$$

with

$$W(k_1,E) = 1 + k_1 E - E^2 = \frac{k_1^2}{4}(1-A^2) + 1. \tag{36}$$

Because the right-hand side of Equation (35) is always greater than or equal to its minimum value k_1 at $s_0 = k_1/2$, we require $W(k_1,E) \geqslant k_1$, so that

$$1 \leqslant E \leqslant k_1 - 1 \tag{37}$$

is the maximum possible energy range of the generated electrons. Because $W \geqslant k_1$, Equation (36) is well approximated by

$$W(k_1,E) = 1 + k_1 E - E^2 = \frac{k_1^2}{4}(1-A^2). \tag{38}$$

Moreover, for soft photon energies $k_2 \ll 1/2$, the upper s-integration limit $k_1 k_2$ in Equation (31) is much smaller than s_0, so we approximate Equation (35) by

$$W(k_1,E) \geqslant \frac{k_1^2}{4s}, \tag{39}$$

providing with approximation (38) the constraint

$$s \geqslant \frac{1}{1-A^2} \geqslant 1, \tag{40}$$

which for all allowed energy values (37) is larger unity. The probability (31) then becomes

$$\begin{aligned} g(E) &\simeq \frac{3\sigma_T}{2k_1^3}\int_0^{2\pi} d\phi \int_{k_1^{-1}}^{1/2}\frac{dk_2}{k_2^2} \\ &\quad \times \int_{\frac{1}{1-A^2}}^{k_1 k_2} ds\, \frac{dn}{dk_2 d\phi d\mu} M(A,s). \end{aligned} \tag{41}$$

Finite values of the last integral only result if

$$\frac{1}{1-A^2} \leqslant k_1 k_2$$

or

$$k_2 \geqslant \frac{1}{k_1(1-A^2)} \geqslant k_1^{-1}. \tag{42}$$

Consequently, we obtain

$$g(E) = \frac{3\sigma_T}{2k_1^3}\int_0^{2\pi} d\phi \int_{\frac{1}{k_1(1-A^2)}}^{1/2} \frac{dk_2}{k_2^2} \times \int_{\frac{1}{1-A^2}}^{k_1 k_2} ds\, \frac{dn}{dk_2 d\phi d\mu} M(A,s). \tag{43}$$

4.1. Gyrotropic and Isotropic Soft Photon Distributions

For the important case of gyrotropic and isotropic soft photon distributions

$$\frac{dn}{dk_2 d\phi d\mu} = \frac{N(k_2)}{4\pi}, \tag{44}$$

the probability (43) reads

$$g(E) = \frac{3\sigma_T}{4k_1^3}\int_{\frac{1}{k_1(1-A^2)}}^{1/2} dk_2\, \frac{N(k_2)}{k_2^2} \times \int_{\frac{1}{1-A^2}}^{k_1 k_2} ds\, M(A,s). \tag{45}$$

Substituting $s = k_1^2 x/4$, we obtain

$$g(E) = \frac{3\sigma_T}{16 k_1}\int_{\frac{1}{k_1(1-A^2)}}^{1/2} dk_2\, \frac{N(k_2)}{k_2^2} I(E,k_1,k_2) \tag{46}$$

with the integrals

$$I(E,k_1,k_2) = \int_{4/k_1^2(1-A^2)}^{4k_2/k_1} dx\, M(A,x) \tag{47}$$

and

$$M(A,x) = \frac{(1-x)^{1/2}}{1-A^2-x}\left[1 + \frac{8}{k_1^2 x} - \frac{32}{k_1^4 x^2} + \frac{A^2}{1-x} - \frac{32A^2}{k_1^4 x^2(1-A^2-x)}\right]. \tag{48}$$

Straightforward, but tedious, integrations, carried out in Appendix A, provide the exact result

$$I(E,k_1,k_2) = R\left[\frac{4k_2}{k_1}\right] - R\left[\frac{4}{k_1^2(1-A^2)}\right], \tag{49}$$

with

$$R[x] = 2(1-x)^{1/2}\left[\frac{16[1-A^2-(A^2+1)x]}{(1-A^2)^2 k_1^4 x(1-A^2-x)} - 1\right] + 4|A|\left[1 + \frac{4}{(1-A^2)k_1^2} - \frac{8(A^2+3)}{(1-A^2)^3 k_1^4}\right] \times \operatorname{artanh}\left(\frac{(1-x)^{1/2}}{|A|}\right) + \frac{16}{(1-A^2)k_1^2}\left[\frac{2(1+3A^2)}{(1-A^2)^2 k_1^2} - 1\right] \times \operatorname{artanh}(1-x)^{1/2}. \tag{50}$$

Instead of using the exact results (49), we approximate the function (48) for small values of $x \leqslant 4k_0/k_1 \ll 1$ by

$$M_0(A,x) = M(A, x \ll 1) = \frac{1}{1-A^2}\left[1 + A^2 + \frac{8}{k_1^2 x} - \frac{32}{k_1^4(1-A^2)x^2}\right]. \tag{51}$$

We readily obtain

$$I(E,k_1,k_2) \simeq \frac{4k_2}{(1-A^2)k_1}\left[\left(1 + A^2 - \frac{2}{k_1 k_2}\right)\left(1 - \frac{1}{k_1 k_2(1-A^2)}\right) + \frac{2}{k_1 k_2}\ln\left[k_1 k_2(1-A^2)\right]\right], \tag{52}$$

so that the electron production probability from a single gamma ray of energy k_1 in gyrotropic and isotropic soft photon distributions becomes

$$g(E) = \frac{3\sigma_T}{4k_1^2(1-A^2)}\int_{\frac{1}{k_1(1-A^2)}}^{1/2} dk_2\, \frac{N(k_2)}{k_2} \times \left[\left(1 + A^2 - \frac{2}{k_1 k_2}\right)\left(1 - \frac{1}{k_1 k_2(1-A^2)}\right) + \frac{2}{k_1 k_2}\ln[k_1 k_2(1-A^2)]\right]. \tag{53}$$

Here the dependence on the electron energy is contained in $A = 1 - (2E/k_1)$. The production spectrum (53) holds for arbitrary soft photon energy distributions $N(k_0)$.

Introducing the electron energy variable

$$y = \frac{E}{k_1/2} - 1 = -A, \tag{54}$$

the probability (53) can be written as

$$g(y) = \frac{3\sigma_T}{4k_1^2(1-y^2)}\int_{\frac{1}{k_1(1-y^2)}}^{1/2} dk_2\, \frac{N(k_2)}{k_2} \times \left[\left(1 + y^2 - \frac{2}{k_1 k_2}\right)\left(1 - \frac{1}{k_1 k_2(1-y^2)}\right) + \frac{2}{k_1 k_2}\ln[k_1 k_2(1-y^2)]\right], \tag{55}$$

which, irrespective of the soft photon energy distributions $N(k_0)$, is symmetric in y, i.e., $g(-y) = g(y)$.

In the following subsections we investigate special soft photon energy distributions.

4.2. Monochromatic Soft Photon Distribution

For the monochromatic soft photon distribution

$$N(k_2) = N_0 \delta(k_2 - k_0) \tag{56}$$

finite values from the general distribution (55) require

$$\frac{1}{k_1(1-y^2)} \leqslant k_0 \leqslant 1/2. \tag{57}$$

The left-hand side of this inequality restricts the allowed electron energies to

$$E_{\min} \leqslant E \leqslant E_{\max} \tag{58}$$

with

$$E_{\rm max,min} = \frac{k_1}{2}\left[1 \pm \sqrt{1 - \frac{1}{k_1 k_0}}\right]. \quad (59)$$

This implies

$$y \in [-m, m], \quad m = \sqrt{1 - \frac{1}{k_1 k_0}}, \quad (60)$$

so that

$$1 - y^2 \in \left[\frac{1}{k_1 k_0}, 1\right]. \quad (61)$$

We find

$$g(-m \leqslant y \leqslant m) = \frac{3\sigma_T N_0}{4k_1^2 k_0 (1-y^2)} H\left[\tfrac{1}{2} - k_0\right] H\left[k_0 - \tfrac{1}{k_1}\right] \times \left[\left(1 + y^2 - \frac{2}{k_1 k_0}\right)\left(1 - \frac{1}{k_1 k_0 (1-y^2)}\right) + \frac{2}{k_1 k_0} \ln\left[k_1 k_0 (1-y^2)\right]\right], \quad (62)$$

or

$$g(E_{\rm min} \leqslant E \leqslant E_{\rm max}) = \frac{3\sigma_T N_0 H\left[\frac{1}{2} - k_0\right] H\left[k_0 - \frac{1}{k_1}\right]}{8 k_0 E(k_1 - E)} \times \left[\frac{1}{k_1 k_0} \ln \frac{4k_0 E(k_1 - E)}{k_1} + \left(\frac{E^2 + (k_1 - E)^2}{k_1^2} - \frac{1}{k_1 k_0}\right) \times \left(1 - \frac{k_1}{4k_0 E(k_1 - E)}\right)\right], \quad (63)$$

which is shown in Figure 3 for the case $k_1 = 10^8$ and $k_0 = 2 \times 10^{-7}$ in comparison with the electron production probability obtained from the numerical Monte Carlo simulation of the electromagnetic cascade described in detail in Elyiv et al. (2009). We did not include the effects of the extragalactic magnetic field as well as the IC interactions with CMB photons, calculating instead only the generated pair energy distribution resulting from the first double photon collisions. As can be seen, the agreement is perfect. The probability exhibits symmetry with respect to $E = (k_1/2)$, and at energies well below k_1 the leading energy dependence of the electron production spectrum is $g(E \ll k_1) \propto E^{-1}$. Moreover, we note that despite its different analytical form, the probability (63) agrees perfectly with the earlier derived expression of Aharonian and coworkers (Aharonian et al. 1983; Aharonian 2003).

4.3. Arbitrary Soft Photon Distribution

For the arbitrary soft photon distribution $N(k_0)$, we find with Equation (63) for the electron production probability from a single gamma-ray photon,

$$n(E, k_1) = \int_0^\infty dk_0 \frac{N(k_0)}{N_0} g\left(E_{\rm min} \leqslant E \leqslant E_{\rm max}\right). \quad (64)$$

The requirement $E_{\rm min} \leqslant E \leqslant E_{\rm max}$ demands

$$k_0 \geqslant \frac{k_1}{4E(k_1 - E)}, \quad (65)$$

so that

$$n(E, k_1) = \frac{3\sigma_T H\left[k_1 - \frac{2E^2}{2E-1}\right]}{8E(k_1 - E)} \int_{\frac{k_1}{4E(k_1-E)}}^{1/2} dk_0 \frac{N(k_0)}{k_0} \times \left[\frac{1}{k_1 k_0} \ln \frac{4k_0 E(k_1 - E)}{k_1} + \left(\frac{E^2 + (k_1 - E)^2}{k_1^2} - \frac{1}{k_1 k_0}\right) \times \left(1 - \frac{k_1}{4k_0 E(k_1 - E)}\right)\right]. \quad (66)$$

Substituting $k_0 = k_1 t/[4E(k_1 - E)]$, we obtain

$$n(E, k_1) = \frac{3\sigma_T H\left[k_1 - \frac{2E^2}{2E-1}\right]}{8k_1^2 E(k_1 - E)} \int_1^{\frac{2E(k_1-E)}{k_1}} \frac{dt}{t} \times N\left(k_0 = \frac{k_1 t}{4E(k_1 - E)}\right)\left[\frac{4E(k_1 - E)}{t}\left(\ln t - 1 + \frac{1}{t}\right) + \left(k_1^2 - 2E(k_1 - E)\right)\left(1 - \frac{1}{t}\right)\right]. \quad (67)$$

The electron energy dependence on $E(k_1 - E)$ guarantees the symmetry of the probability dependence, generated by a single gamma ray, around $E = k_1/2$ for arbitrary soft photon distributions.

4.4. Pair Density

The number of pairs with energy E created per unit length path depends on the electron production probability (67) and on the probability of the incoming gamma rays remaining unabsorbed up to the point of observation (Cerutti et al. 2009)

$$\frac{dN_e}{dl dE} = 2n(E, k_1) e^{-\tau(k_1, l)}, \quad (68)$$

with the optical depth

$$\frac{d\tau(k_1, l)}{dl} = \int_0^\infty dE\, n(E, k_1), \quad (69)$$

so that the integration of Equation (68) over all electron energies provides

$$\frac{dN_e}{dl} = 2\frac{d\tau(k_1, l)}{dl} e^{-\tau(k_1, l)}. \quad (70)$$

The total number of pairs produced by a single gamma ray traversing a soft photon radiation field along the path l up to the distance r then is

$$N_e(k_1, r) = 2[1 - e^{-\tau(k_1, r)}] \simeq \begin{cases} 2\tau(k_1, r) & \text{for } \tau(k_1, r) \ll 1 \\ 2 & \text{for } \tau(k_1, r) \gg 1. \end{cases} \quad (71)$$

A differential gamma-ray photon spectrum $I_1(k_1)$ in units of photons cm^{-2} s^{-1} eV^{-1} corresponds to the gamma-ray photon density $m_e c^2 k_1 I_1(k_1)/c$, implying for the number density of produced pairs

$$n_e(k_1, r) = \frac{m_e c^2 k_1 I_1(k_1) N_e(k_1, r)}{c} = \frac{2 m_e c^2 k_1 I_1(k_1)}{c}[1 - e^{-\tau(k_1, r)}]. \quad (72)$$

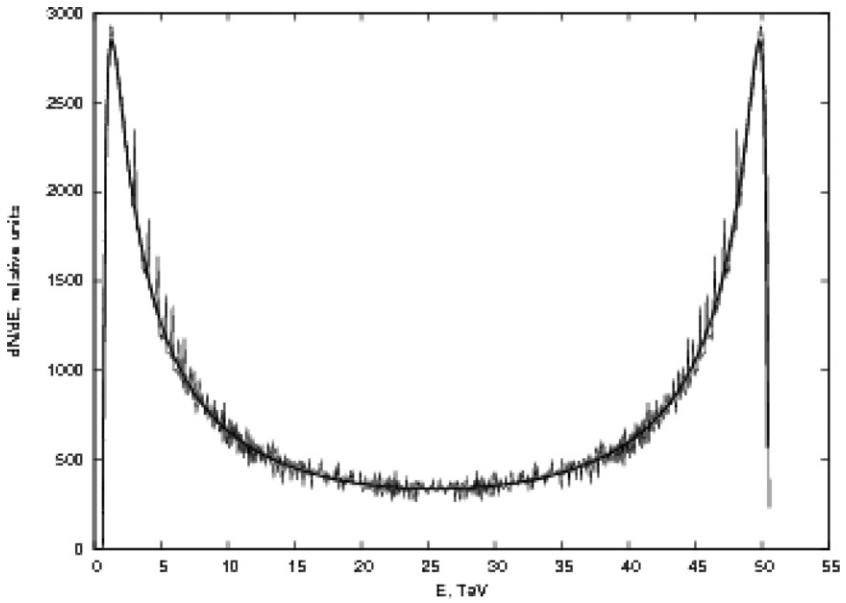

Figure 3. Probability of a single gamma ray of energy $k_1 = 10^8$ (corresponding to 51.1 TeV) being absorbed between the path length l and $l + dl$, yielding an electron of energy between E and $E + dE$, when interacting with monoenergetic isotropically distributed soft photons $k_0 = 2 \times 10^{-7}$ (corresponding 0.1 eV) of EBL. The analytical result (63) (thick line) agrees perfectly with the result from the numerical simulations (thin line). The simulations were done for the same conditions using the Monte Carlo method detailed in Elyiv et al. (2009).

For spatially uniformly distributed soft photon distribution, the optical depth is given by

$$\tau(k_1, r) = r \int_0^\infty dE\, n(E, k_1). \tag{73}$$

Likewise, the integration of Equation (68) over all path lengths yields the differential energy spectrum of the produced pairs from a single gamma ray traversing a soft photon radiation field along the path l up to the distance r as

$$\begin{aligned}\frac{dN_e}{dE}(E, k_1, r) &= 2n(E, k_1) \int_0^r dl\, \exp\left[-l \int_0^\infty dE\, n(E, k_1)\right] \\ &= \frac{2rn(E, k_1)}{\tau(k_1, r)}[1 - e^{-\tau(k_1, r)}] \\ &= N_e(k_1, r) \frac{n(E, k_1)}{\int_0^\infty dE\, n(E, k_1)} \\ &\simeq \begin{cases} 2rn(E, k_1) & \text{for } \tau(\mathrm{k_1}, \mathrm{r}) \ll 1 \\ \frac{2rn(E, k_1)}{\tau(k_1, r)} & \text{for } \tau(\mathrm{k_1}, \mathrm{r}) \gg 1. \end{cases}\end{aligned} \tag{74}$$

5. SINGLE GAMMA-RAY PAIR PRODUCTION OPTICAL DEPTH

The calculation of the optical depth (73) of a single gamma-ray photon requires the integration of Equation (66) over all electron energies

$$\begin{aligned}\tau(k_1, r) &= r \int_{E_{\min}}^{E_{\max}} dE \int_0^\infty dk_0 \frac{N(k_0)}{N_0} g\,(E_{\min} \leqslant E \leqslant E_{\max}) \\ &= \frac{3\sigma_T r}{8} \int_{E_{\min}}^{E_{\max}} \frac{dE}{E(k_1 - E)} \int_{\frac{k_1}{4E(k_1 - E)}}^{1/2} dk_0 \frac{N(k_0)}{k_0} \\ &\quad \times \left[\frac{1}{k_1 k_0} \ln \frac{4k_0 E(k_1 - E)}{k_1}\right. \\ &\quad \left. + \left(\frac{E^2 + (k_1 - E)^2}{k_1^2} - \frac{1}{k_1 k_0}\right) \right. \\ &\quad \left. \times \left(1 - \frac{k_1}{4k_0 E(k_1 - E)}\right)\right].\end{aligned} \tag{75}$$

Using the electron energy variable (54) and Equation (60), we obtain

$$\tau(k_1, r) = \frac{3\sigma_T r H[k_1 - 2]}{4k_1} \int_{k_1^{-1}}^{1/2} dk_0 \frac{N(k_0)}{k_0} \int_0^m dy\, K(y) \tag{76}$$

with the function

$$\begin{aligned}K(y) = \frac{1}{1 - y^2}\Big(&1 + m^2 - 2(1 - m^2)\ln(1 - m^2) - (1 - y^2) \\ &- \frac{2m^2(1 - m^2)}{1 - y^2} + 2(1 - m^2)\ln(1 - y^2)\Big).\end{aligned} \tag{77}$$

The step function in Equation (76) arises from the condition that $k_1^{-1} \leqslant (1/2)$. Using

$$\int_0^m \frac{dy}{(1 - y^2)^2} = \frac{1}{2}\left[\frac{m}{1 - m^2} + \operatorname{artanh} m\right] \tag{78}$$

and the integral (evaluated in Appendix B)

$$\begin{aligned}I_7(m) &= \int_0^m dy \frac{\ln(1 - y^2)}{(1 - y^2)} \\ &= \frac{1}{4}[\ln^2(1 + m) - \ln^2(1 - m) + 2\ln(1 - m)\ln(1 + m)] \\ &\quad - \ln 2 \ln(1 + m) - \mathrm{Li}\left[\frac{1}{2}, \frac{1 + m}{2}\right]\end{aligned} \tag{79}$$

with the dilogarithm (Abramowitz & Stegun 1972)

$$\mathrm{Li}[a, b] = \int_a^b ds \frac{\ln(1 + s)}{s}, \tag{80}$$

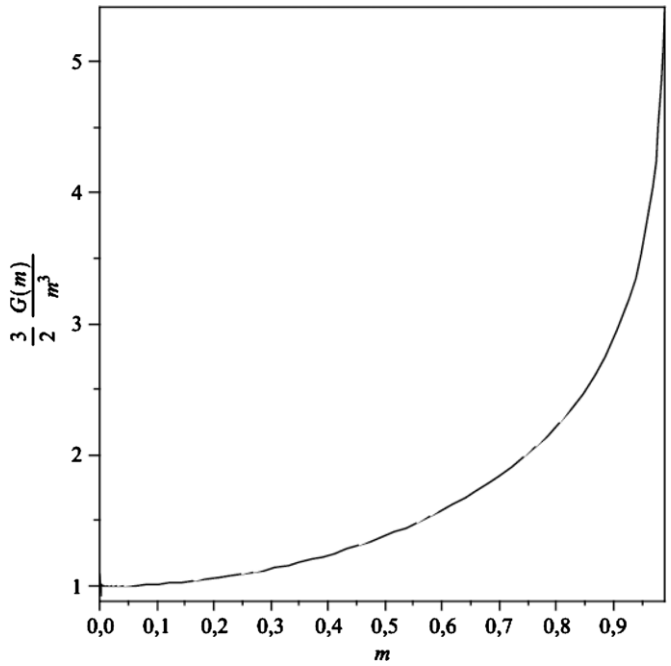

Figure 4. Ratio between the exact variation (82) and its lowest order approximation (84) of the function $G(m)$.

which cannot be expressed as a finite combination of elementary functions (Gradshteyn & Ryzhik 1980), we obtain

$$\tau(k_1, r) = \frac{3\sigma_T r H[k_1 - 2]}{4k_1} \int_{k_1^{-1}}^{1/2} dk_0 \frac{N(k_0)}{k_0} G(m) \tag{81}$$

with

$$\begin{aligned} G(m) &= \int_0^m dy\, K(y) \\ &= [1 + m^4 - 2(1-m^2)\ln(1-m^2)]\operatorname{artanh} m \\ &\quad - m(1+m^2) + 2(1-m^2) I_7(m). \end{aligned} \tag{82}$$

Substituting in Equation (81) m from Equation (60), we find

$$\begin{aligned} \tau(k_1, r) = &\frac{3\sigma_T r H[k_1 - 2]}{2k_1} \\ &\times \int_0^{\sqrt{1-\frac{2}{k_1}}} dm\, \frac{m G(m)}{1-m^2} N\left(\frac{1}{k_1(1-m^2)}\right). \end{aligned} \tag{83}$$

For small values of $m \ll 1$, we note the asymptotic behavior

$$G(m \ll 1) \simeq \frac{2}{3} m^3 \left[1 + \frac{7}{5} m^2\right]. \tag{84}$$

As Figure 4 illustrates, this approximations agrees reasonable well with the exact variation $G(m)$ for all values of $m < 1$, so that we use it to find for the optical depth (83)

$$\begin{aligned} \tau(k_1, r) \simeq &\frac{\sigma_T r H[k_1 - 2]}{k_1} \int_0^{\sqrt{1-\frac{2}{k_1}}} dm\, \frac{m^4}{1-m^2} N \\ &\times \left(\frac{1}{k_1(1-m^2)}\right). \end{aligned} \tag{85}$$

5.1. Wien-type Soft Photon Distribution

We now specify the soft photon distribution by the generalized Wien-type spectrum

$$N_W(k_0) = \frac{N_0}{\Gamma(q+1)\Theta^{1+q}} k_0^q e^{-k_0/\Theta}, \tag{86}$$

characterized by its power-law index $q > -1$ and the dimensionless temperature $\Theta = k_b T_W / m_e c^2$. N_0 denotes the total number of soft photons and $\Gamma(x)$ denotes the Gamma function. For the optical depth (85) we then derive

$$\begin{aligned} \tau(k_1, r) \simeq &\frac{\sigma_T N_0 r H[k_1 - 2]}{\Gamma(q+1)(\Theta k_1)^{q+1}} \int_0^{\sqrt{1-\frac{2}{k_1}}} dm \\ &\times \frac{m^4}{(1-m^2)^{q+1}} e^{-\frac{1}{\Theta k_1 (1-m^2)}}. \end{aligned} \tag{87}$$

The substitution $t = 1/(1-m^2)$ provides

$$\tau(k_1, r) \simeq \frac{\sigma_T N_0 r H[k_1 - 2]}{2\Gamma(q+1)(\Theta k_1)^{q+1}} \Omega(\Theta, k_1, q) \tag{88}$$

with the integral

$$\begin{aligned} \Omega(\Theta, k_1, q) &= \int_1^{k_1/2} dt\, (t-1)^{3/2} t^{q-5/2} e^{-\frac{t}{\Theta k_1}} \\ &= \Gamma\left(\frac{5}{2}\right) e^{-\frac{1}{\Theta k_1}} U\left(\frac{5}{2}, q+1, \frac{1}{\Theta k_1}\right) \\ &\quad - \int_{k_1/2}^{\infty} dt\, (t-1)^{3/2} t^{q-5/2} e^{-\frac{t}{\Theta k_1}} \end{aligned} \tag{89}$$

expressed in terms of the confluent hypergeometric function of the second kind (Abramowitz & Stegun 1972). For values $k_1 \gg 2$ the remaining integral is approximated as

$$\begin{aligned} \int_{k_1/2}^{\infty} dt\, (t-1)^{3/2} t^{q-5/2} e^{-\frac{t}{\Theta k_1}} &\simeq \int_{k_1/2}^{\infty} dt\, t^{q-1} e^{-\frac{t}{\Theta k_1}} \\ &= (\Theta k_1)^q \int_{\frac{1}{2\Theta}}^{\infty} ds\, s^{q-1} e^{-s} \\ &\simeq (\Theta k_1)^q (2\Theta)^{1-q} e^{-\frac{1}{2\Theta}} \\ &= 2^{1-q} \Theta k_1^q e^{-\frac{1}{2\Theta}} \ll 1, \end{aligned} \tag{90}$$

where in the penultimate step we used the smallness of $\Theta \ll 1$. This contribution is negligibly small. We then obtain

$$\Omega(\Theta, k_1, q > 1) \simeq \Gamma\left(\frac{5}{2}\right) e^{-\frac{1}{\Theta k_1}} U\left(\frac{5}{2}, q+1, \frac{1}{\Theta k_1}\right), \tag{91}$$

providing for the optical depth (88)

$$\tau(k_1, r) \simeq \frac{\Gamma(5/2)\sigma_T N_0 r H[k_1 - 2]}{2\Gamma(q+1)(\Theta k_1)^{q+1}} e^{-\frac{1}{\Theta k_1}} U\left(\frac{5}{2}, q+1, \frac{1}{\Theta k_1}\right). \tag{92}$$

For small gamma-ray energies $k_1 \ll \Theta^{-1}$, we obtain the approximation

$$\tau(k_1 \ll \Theta^{-1}, r) \simeq \frac{\Gamma(5/2)\sigma_T N_0 r H[k_1 - 2]}{2\Gamma(q+1)} (\Theta k_1)^{\frac{3}{2}-q} e^{-\frac{1}{\Theta k_1}}. \tag{93}$$

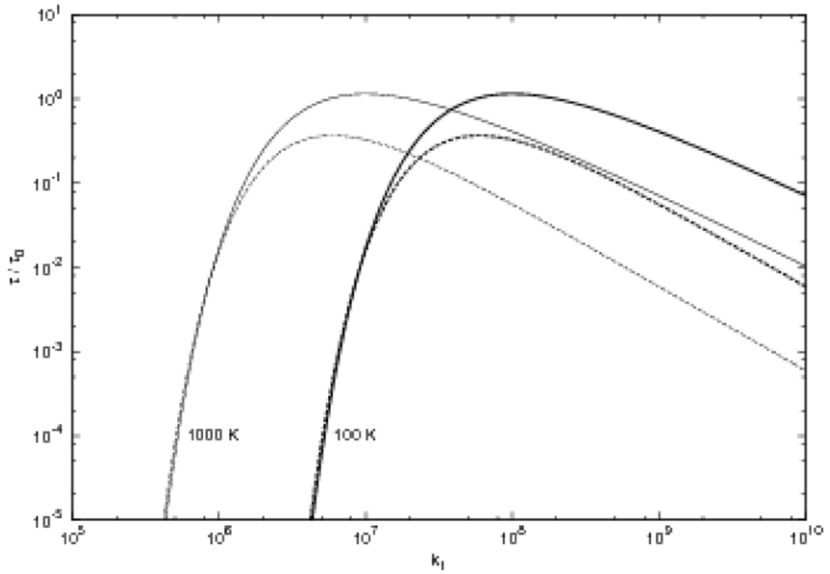

Figure 5. Comparison of the analytical approximation (96) of the optical depth (dashed lines) with the numerically calculated one (solid lines) for a Wien-type soft photon distribution with $q = 2$ and two temperatures $T_W = 100$ and 1000 K.

This is reduced exponentially because for these gamma-ray energies only soft photons in the exponential tail of the Wien distribution overcome the threshold for pair production.

For large gamma-ray energies $k_1 \gg \Theta^{-1}$ the asymptotic behavior of the confluent hypergeometric function depends on the power-law index value q of the Wien distribution, or

$$U\left(\frac{5}{2}, q+1, \frac{1}{\Theta k_1}\right) \simeq \begin{cases} \frac{\Gamma(q)}{\Gamma(5/2)(\Theta k_1)^q} & \text{for q} > 0 \\ \frac{1}{\Gamma(5/2)}[\ln(\Theta k_1) - 2.258] & \text{for q} = 0 \\ \frac{1}{\Gamma(7/2)} & \text{for q} = -1 \\ \frac{\Gamma(-q)}{\Gamma\left(\frac{5}{2}-q\right)} & \text{for} -1 < |\text{q}| < 0. \end{cases} \quad (94)$$

For the corresponding optical depth at large photon energies, we then obtain

$$\tau(k_1 \gg \Theta^{-1}, r) \simeq \frac{\sigma_T N_0 r H[k_1 - 2]}{2\Gamma(q+1)(\Theta k_1)^{1+q}} \times \begin{cases} \Gamma(q)(\Theta k_1)^q & \text{for } q > 0 \\ [\ln(\Theta k_1) - 2.258] & \text{for } q = 0 \\ \frac{2}{5} & \text{for } q = -1 \\ \frac{\Gamma(-q)\Gamma(\frac{5}{2})}{\Gamma(\frac{5}{2}-q)} & \text{for } -1 < |q| < 0. \end{cases} \quad (95)$$

For values of $q > 0$, we use the approximation

$$\tau(k_1, r) \simeq \frac{\tau_0}{\Theta k_1 e^{\frac{1}{\Theta k_1}}} \quad (96)$$

with

$$\tau_0 = \frac{\sigma_T N_0 r H[k_1 - 2]}{2q} \quad (97)$$

at all gamma-ray energies. In Figure 5, we compare the analytical single gamma-ray pair optical depth (96) with the numerically calculated one, using the cross section from Aharonian (2003) and Wien-type soft photon distribution with $q = 2$ and the two temperatures $T_W = 100$ K and $T_W = 1000$ K. As can be seen, the agreement is very good for gamma-ray energies below the maximum optical depth. At higher energies the dependences on photon energy agree well, although the analytical calculations underestimate the numerical values by a factor 3–10.

6. ARBITRARY GAMMA-RAY ENERGY DISTRIBUTION

For an extended differential gamma-ray number density distribution $I(k_1) = m_e c^2 I_1(k_1)$ below the maximum energy $k_1 \leqslant k_{1,\max} = M$, now in units of photons per $\text{cm}^{-2}\,\text{s}^{-1}(dk_1)^{-1}$, we obtain with Equation (74) the differential energy spectrum of the produced pairs at the distance r as

$$\frac{dN_e}{dE}(E, r) = \int_0^M dk_1\, I(k_1) \frac{dN_e}{dE}(E, k_1, r) = 2r \int_0^M dk_1\, I(k_1) n(E, k_1) \frac{1 - e^{-\tau(k_1, r)}}{\tau(k_1, r)}. \quad (98)$$

Inserting Equation (67) then provides

$$\frac{dN_e}{dE}(E, r) = \frac{3r\sigma_T}{4} \int_{\frac{2E^2}{2E-1}}^M \frac{dk_1}{k_1^2} I(k_1) \frac{1 - e^{-\tau(k_1, r)}}{\tau(k_1, r)} \times \left[4 \int_1^{2E(1-\frac{E}{k_1})} dt\, N\left(\frac{t}{4E\left(1 - \frac{E}{k_1}\right)}\right) \times \frac{\ln t + t^{-1} - 1}{t^2} + \left[\frac{k_1}{E\left(1 - \frac{E}{k_1}\right)} - 2\right] \times \int_1^{2E(1-\frac{E}{k_1})} dt\, N\left(\frac{t}{4E\left(1 - \frac{E}{k_1}\right)}\right) \frac{t-1}{t^2}\right]. \quad (99)$$

Provided the maximum gamma-ray energy $M \geqslant 2$, electrons are produced in the energy range

$$\frac{M}{2}\left[1 - \sqrt{1 - \frac{2}{M}}\right] \leqslant E \leqslant \frac{M}{2}\left[1 + \sqrt{1 - \frac{2}{M}}\right]. \quad (100)$$

Equation (99) is the general analytical expression of the energy spectrum of electrons produced from the annihilation interactions of a beam of high-energy gamma rays with arbitrary differential number density distribution $I(k_1)$ below $k_1 \leqslant M$ with an isotropically distributed soft photon gas with arbitrary differential number density distribution $N(k_0)$.

6.1. Power-law-distributed Gamma Rays

Blazar observations often indicate power-law distributions of the emitted gamma-ray beam with $I(k_1) = I_0 k_1^{-p}$ for $k_1 \leqslant M$. In this case the electron spectrum (99) reduces to

$$\frac{dN_e}{dE}(E,r) = \frac{3r\sigma_T I_0}{4}\int_{\frac{2E^2}{2E-1}}^{M} dk_1\, k_1^{-(p+2)}\frac{1-e^{-\tau(k_1,r)}}{\tau(k_1,r)} \times\left[4\int_1^{2E(1-\frac{E}{k_1})} dt\, N\left(\frac{t}{4E\left(1-\frac{E}{k_1}\right)}\right) \times\frac{\ln t + t^{-1}-1}{t^2} + \left[\frac{k_1}{E\left(1-\frac{E}{k_1}\right)}-2\right] \times\int_1^{2E(1-\frac{E}{k_1})} dt\, N\left(\frac{t}{4E\left(1-\frac{E}{k_1}\right)}\right)\frac{t-1}{t^2}\right]. \tag{101}$$

In the next section, we will investigate the astrophysically relevant soft photon Wien energy distribution (86) with spectral index $q > 0$.

7. WIEN-TYPE SOFT PHOTON DISTRIBUTION AND POWER-LAW-DISTRIBUTED GAMMA RAYS

7.1. Optical Depth Influence

We first approximate the factor

$$\frac{1-e^{-\tau(k_1,r)}}{\tau(k_1,r)} \simeq \frac{1}{1+\tau(k_1,r)} \tag{102}$$

for all values of τ, noting that for $\tau \ll 1$ and $\tau \gg 1$ the left-hand and right-hand sides of Equation (102) approach the same values 1 and τ^{-1}, respectively. Limiting our discussion to Wien distributions with $q > 1$, the optical depth (96) then provides

$$\frac{1-e^{-\tau(k_1,r)}}{\tau(k_1,r)} \simeq \frac{1}{1+\tau(\Theta k_1)} \tag{103}$$

with

$$\tau(x) = \tau_0 x^{-1} e^{-\frac{1}{x}} \simeq \tau_0\begin{cases} e^{-x^{-1}} & \text{for } x \ll 1 \\ x^{-1} & \text{for } x \gg 1. \end{cases} \tag{104}$$

The function $\tau(x)$ attains its maximum value $\tau_{\max} = \tau_0 e^{-1} = 0.37\tau_0$ at $x = 1$, is exponentially reduced at small values of x, and decreases proportional to x^{-1} at large values of x.

The limit of large path length

$$r \gg r_0 = (N_0\sigma_T)^{-1} = \frac{0.49}{N_0}\ \text{Mpc}, \tag{105}$$

where $N_0^{\rm EBL} \simeq 1$ is of order unity, corresponds to values of $\tau_0 \gg 1$, so that the factor (103) varies approximately as

$$\frac{1}{1+\tau(x)} \simeq \begin{cases} 1 & \text{for } x \leqslant \frac{1}{\ln\tau_0} \\ \frac{xe^{\frac{1}{x}}}{\tau_0} & \text{for } \frac{1}{\ln\tau_0} \leqslant x \leqslant \tau_0 \\ 1 & \text{for } x > \tau_0. \end{cases} \tag{106}$$

7.2. Further Reduction of the Electron Spectrum

Substituting $k_1 = Ez/(z-1)$, we obtain for the electron spectrum (101)

$$\frac{dN_e}{dE}(E,r) = \frac{3r\sigma_T I_0 H[M-2]}{4E^{1+p}}\int_{\frac{M}{M-E}}^{2E}\frac{dz}{z^2}\frac{\left(1-\frac{1}{z}\right)^p}{1+\tau(k_1(z),r)} \times\left[4\int_1^{\frac{2E}{z}} dt\, N\left(\frac{zt}{4E}\right)\frac{\ln t + t^{-1}-1}{t^2} + \frac{z^2-2z+2}{z-1}\int_1^{\frac{2E}{z}} dt\, N\left(\frac{zt}{4E}\right)\frac{t-1}{t^2}\right]. \tag{107}$$

Using the Wien distribution (86), we find

$$\frac{dN_e}{dE}(E,r) = \frac{3r\sigma_T I_0 N_0 H[M-2]}{4^{q+1}\Gamma(1+q)\Theta^{1+q}E^{1+q+p}} \times\int_{\frac{1}{1-\frac{E}{M}}}^{2E} dz\, e^{-\frac{z}{4\Theta E}}\frac{z^{q-2}\left(1-\frac{1}{z}\right)^p}{1+\tau_0\left(\frac{1-\frac{1}{z}}{\Theta E}\right)e^{-\frac{1-\frac{1}{z}}{\Theta E}}} J(E,\Theta,z) \tag{108}$$

with the integral

$$J(E,\Theta,z) = 4\int_0^{\frac{2E}{z}-1} dy\,(1+y)^{q-3}[(1+y)\ln(1+y)-y]e^{-\frac{zy}{4\Theta E}} + \frac{z^2-2z+2}{z-1}\int_0^{\frac{2E}{z}-1} dy\, y(1+y)^{q-2}e^{-\frac{zy}{4\Theta E}}, \tag{109}$$

where we substituted $t = 1+y$ in the two second integrals of Equation (107). Using Equation (97) for the factor $r\sigma_T N_0$, we obtain

$$\frac{dN_e}{dE}(E,r) = \frac{3\tau_0 I_0 H[M-2]}{2^{2q-1}\Gamma(q)\Theta^{1+q}E^{1+q+p}} \times\int_{\frac{1}{1-\frac{E}{M}}}^{2E} dz\,\frac{z^{q-2}\left(1-\frac{1}{z}\right)^p e^{-\frac{z}{4\Theta E}}}{1+\tau_0\left(\frac{1-\frac{1}{z}}{\Theta E}\right)e^{-\frac{1-\frac{1}{z}}{\Theta E}}} J(E,\Theta,z). \tag{110}$$

The most interesting feature of this equation is the dependence on τ_0. For distant blazars with luminosity distances $d_L \gg r_0 \simeq 0.49N_0^{-1}$ Mpc, τ_0 attains values larger than 10^3, so that one could take the formal limit of $\tau_0 \to \infty$. In this limit the τ_0-dependence of the spectrum (110) cancels out, providing

$$\frac{dN_e}{dE}(E,\tau_0 \gg 1) = \frac{3I_0 H[M-2]e^{\frac{1}{\Theta E}}}{2^{2q+1}\Gamma(q)\Theta^q E^{q+p}} \times\int_{\frac{1}{1-\frac{E}{M}}}^{2E} dz\, z^{q-2}\left(1-\frac{1}{z}\right)^{p-1} e^{-\frac{\frac{4}{z}+z}{4\Theta E}} J(E,\Theta,z) \tag{111}$$

subject to the additional constraint from $\tau(E,z) > 1$ and, implying from Equation (106),

$$\frac{1}{\ln\tau_0} \leqslant \frac{\Theta E}{1-\frac{1}{z}} \leqslant \tau_0. \tag{112}$$

Because $z \geqslant 2$ for all values of E, we ignore the small z-dependence of this constraint, which then provides the electron energy restriction

$$\frac{1}{\Theta \ln \tau_0} \leqslant E \leqslant \frac{\tau_0}{\Theta} \tag{113}$$

for the spectrum (111), i.e.,

$$\frac{dN_e}{dE}\left(\frac{1}{\Theta \ln \tau_0} \leqslant E \leqslant \frac{\tau_0}{\Theta}, \tau_0 \gg 1\right) \simeq \frac{3I_0 H[M-2] e^{\frac{1}{\Theta E}}}{2^{2q+1}\Gamma(q)\Theta^q E^{q+p}} \times \int_{\frac{1}{1-\frac{E}{M}}}^{2E} dz\, z^{q-2}\left(1-\frac{1}{z}\right)^{p-1} e^{-\frac{\frac{4}{3}+z}{4\Theta E}} J(E,\Theta,z). \tag{114}$$

This energy spectrum is only determined by the number (I_0) of incoming gamma rays and independent on the actual value of τ_0, if this is large enough. This behavior reflects the fact that any incoming single gamma ray can at most produce only two electrons.

Outside of the energy interval (113) we neglect the τ_0-dependence under the integral in Equation (110) and obtain

$$\frac{dN_e}{dE}\left(E \leqslant \frac{1}{\Theta \ln \tau_0}, \tau_0 \gg 1\right) = \frac{dN_e}{dE}\left(E > \frac{\tau_0}{\Theta}, \tau_0 \gg 1\right) = \frac{3\tau_0 I_0 H[M-2]}{2^{2q+1}\Gamma(q)\Theta^{1+q}E^{1+q+p}} \int_{\frac{1}{1-\frac{E}{M}}}^{2E} dz\, z^{q-2}\left(1-\frac{1}{z}\right)^p e^{\frac{-z}{4\Theta E}} J(E,\Theta,z). \tag{115}$$

Here the production spectrum increases with τ_0 as the electrons are produced by gamma rays with energies such that $\tau(\Theta k_1) < 1$.

Both electron production spectra (114) and (115) depend on the same integral $J(E,\Theta,z)$ that we evaluate approximately in Appendix C as

$$J(E,\Theta,z) \simeq \left[z-1+\frac{1}{z-1}\right]\begin{cases}\frac{\alpha^2}{2} & \text{for } \alpha \ll 1\\ \frac{\alpha^q}{q} & \text{for } \alpha \gg 1,\end{cases} \tag{116}$$

where

$$\alpha = \frac{4\Theta E}{z}. \tag{117}$$

8. ELECTRON PRODUCTION SPECTRA

In this section we calculate the electron production spectra for electron energies outside and inside the interval $[1/\Theta \ln \tau_0, \tau_0/\Theta]$.

The electron production spectra (115) is determined by the last remaining integral

$$T_1(E,\Theta) = \int_{\frac{1}{1-\frac{E}{M}}}^{2E} dz\, z^{q-2}\left(1-\frac{1}{z}\right)^p e^{-\frac{z}{4\Theta E}} J\left(\frac{4\Theta E}{z}\right). \tag{118}$$

With the asymptotics (116) we find

$$T_1(E,\Theta) \simeq \int_{\frac{M}{M-E}}^{2E} dz\, z^{q-(2+p)}[(z-1)^{p+1}+(z-1)^{p-1}] \times \left[\frac{(4\Theta E)^q}{q z^q} H[4\Theta E - z] + \frac{(4\Theta E)^2}{2z^2} H[z-4\Theta E]\right] e^{-\frac{z}{4\Theta E}}. \tag{119}$$

Because the upper integration limit $2E$ is always larger than $4\Theta E$ for $\Theta < (1/2)$, the behavior of Equation (119) depends on the value of $4\Theta E$ in comparison to the lower ($L = M/(M-E) \geqslant 2$) integration limit. We introduce their ratio as the function

$$X(E) = \frac{L}{4\Theta E} = \frac{M}{4\Theta E(M-E)}. \tag{120}$$

For electron energy values $E \ll \Theta^{-1}$, regardless of the value of M, we always have $4\Theta E \ll L$, corresponding to $X \gg 1$, so that

$$T_1(E \ll \Theta^{-1}) \simeq \frac{(4\Theta E)^2}{2} H[X-1] \int_{\frac{M}{M-E}}^{2E} dz\, z^{q-(4+p)} \times [(z-1)^{p+1}+(z-1)^{p-1}] e^{-\frac{z}{4\Theta E}}. \tag{121}$$

Likewise, for large electron energies $\Theta^{-1} \ll E < M$, we find

$$T_1(E \gg \Theta^{-1}) \simeq H[1-X] \times \left(\frac{(4\Theta E)^2}{2}\int_{4\Theta E}^{2E} dz\, z^{q-(4+p)}[(z-1)^{p+1}+(z-1)^{p-1}] e^{-\frac{z}{4\Theta E}} + \frac{(4\Theta E)^q}{q}\int_{\frac{M}{M-E}}^{4\Theta E} dz\, z^{-(2+p)}[(z-1)^{p+1}+(z-1)^{p-1}]\right), \tag{122}$$

where in the second term we approximated $\exp[-z/(4\Theta E)] \simeq 1$.

For the following analysis it is convenient to introduce the dimensionless electron energy variable

$$E = \frac{M}{2}\epsilon, \tag{123}$$

where, according to Equation (100),

$$1-\sqrt{1-\frac{2}{M}} \leqslant \epsilon \leqslant 1+\sqrt{1-\frac{2}{M}}. \tag{124}$$

The function (120) reads

$$X(\epsilon) = \frac{1}{\Theta M \epsilon(2-\epsilon)}. \tag{125}$$

The function $X(\epsilon)$ is symmetric with respect to $\epsilon = 1$, where it attains its minimum value

$$X_{\min} = \frac{1}{\Theta M}. \tag{126}$$

At the minimum and maximum electron energies (125), $X(\epsilon_{\min,\max}) = X_{\max} = 1/(2\Theta) \gg 1$.

Likewise, the electron production spectrum (115) becomes

$$\frac{dN}{d\epsilon}(\epsilon) = \frac{3\tau_0 I_0 H[M-2]}{2^{q-p+1}\Gamma(q)\Theta^{1+q}M^{q+p}\epsilon^{1+q+p}} T_1(\epsilon), \tag{127}$$

with

$$T_1\left(\epsilon \ll \frac{2}{M\Theta}\right) \simeq 2(\Theta M\epsilon)^2 H[X-1] \times \int_{\frac{2}{2-\epsilon}}^{M\epsilon} dz\, z^{q-(4+p)}[(z-1)^{p+1}+(z-1)^{p-1}] e^{-\frac{z}{2\Theta M\epsilon}} \tag{128}$$

and

$$T_1\left(\epsilon \gg \frac{2}{M\Theta}\right) \simeq H[1-X] \times \left(\frac{(2\Theta M\epsilon)^2}{2}\int_{2\Theta M\epsilon}^{M\epsilon} dz\, z^{q-(4+p)}[(z-1)^{p+1}+(z-1)^{p-1}]e^{-\frac{z}{2\Theta M\epsilon}} + \frac{(2\Theta M\epsilon)^q}{q}\int_{\frac{2}{2-\epsilon}}^{2\Theta M\epsilon} dz\, z^{-(2+p)}[(z-1)^{p+1}+(z-1)^{p-1}]\right). \quad (129)$$

In terms of ϵ the overriding energy restrictions $E \leqslant (1/\Theta \ln\tau_0)$ and $E > \tau_0/\Theta$ correspond to

$$\epsilon \leqslant \frac{2}{M\Theta\ln\tau_0} < \frac{2}{M\Theta}, \quad (130)$$

provided $\ln\tau_0 > 1$, and

$$\epsilon > \frac{2\tau_0}{M\Theta} > \frac{2}{M\Theta}, \quad (131)$$

provided $\tau_0 > 1$.

8.1. Electron Production Spectrum for $E \ll (\Theta\ln\tau_0)^{-1}$

Here we substitute in Equation (128) $z = t/(1-(\epsilon/2))$ to obtain

$$\begin{aligned} V_1(\epsilon) &= \frac{T_1\left(\epsilon \ll \frac{2}{M\Theta}\right)H[X-1])}{2(\Theta M\epsilon)^2} \\ &= \left(1-\frac{\epsilon}{2}\right)^{3+p-q}\int_1^{\frac{1}{2\Theta X}} dt\, t^{q-(4+p)} \times\left[\left(\frac{t}{1-\frac{\epsilon}{2}}-1\right)^{p+1}+\left(\frac{t}{1-\frac{\epsilon}{2}}-1\right)^{p-1}\right]e^{-Xt} \\ &= \left(1-\frac{\epsilon}{2}\right)^{2-q}e^{-X}\int_0^{\frac{1}{2\Theta X}-1} dy\,(1+y)^{q-(4+p)} \times\left[\left(y+\frac{\epsilon}{2}\right)^{p+1}+\left(1-\frac{\epsilon}{2}\right)^2\left(y+\frac{\epsilon}{2}\right)^{p-1}\right]e^{-Xy}, \end{aligned} \quad (132)$$

where we substituted $t = 1+y$ in the last step. Replacing the exponential function by unity for $y < X^{-1} < 1$ and zero otherwise, we obtain to leading order in $(1/X)$,

$$\begin{aligned} V_1(\epsilon) &\simeq \left(\frac{\epsilon}{2}\right)^p\left(1-\frac{\epsilon}{2}\right)^{2-q}e^{-X} \times\left[\left(\frac{\epsilon}{2}\right)^2\frac{\left(1+\frac{2}{\epsilon X}\right)^{p+2}-1}{p+2}+\left(1-\frac{\epsilon}{2}\right)^2\frac{\left(1+\frac{2}{\epsilon X}\right)^p-1}{p}\right] \\ &= \left(\frac{\epsilon}{2}\right)^p\left(1-\frac{\epsilon}{2}\right)^{2-q}e^{-X}\left[\left(\frac{\epsilon}{2}\right)^2\frac{(1+2\Theta M(2-\epsilon))^{p+2}-1}{p+2} +\left(1-\frac{\epsilon}{2}\right)^2\frac{(1+2\Theta M(2-\epsilon))^p-1}{p}\right]. \end{aligned} \quad (133)$$

With Equations (132) we then obtain for the electron production spectrum at small energies

$$\frac{dN}{d\epsilon}\left(\epsilon \ll \frac{2}{M\Theta\ln\tau_0}\right) \simeq \frac{3\tau_0 I_0}{4\Gamma(q)M^p\Theta} \times X^{q-2}e^{-X}H[X-1]Y(\epsilon) \quad (134)$$

with the function

$$Y(\epsilon) = \epsilon^{-1}\left[\left(\frac{\epsilon}{2}\right)^2\frac{(1+2\Theta M(2-\epsilon))^{p+2}-1}{p+2} +\left(1-\frac{\epsilon}{2}\right)^2\frac{(1+2\Theta M(2-\epsilon))^p-1}{p}\right]. \quad (135)$$

The production spectrum (134) at low electron energies is the product of a power law with an exponential cutoff in the symmetric energy variable $X(E)$, which reflects the adopted Wien soft photon spectrum, times the distribution function $Y(\epsilon)$, which reflects the incoming gamma-ray power-law distribution.

Depending on the maximum gamma-ray energy M being smaller or larger than Θ^{-1}, we derive its approximations as

$$Y(\epsilon, M\Theta \ll 1) \simeq \frac{1}{X}\left[1-\frac{2}{\epsilon}+\frac{2}{\epsilon^2}\right] \quad (136)$$

(independent of the incoming gamma-ray energy distribution) and

$$Y(\epsilon, M\Theta \gg 1) \simeq \frac{2^p}{p+2}\epsilon^{-(1+p)}X^{-(p+2)} \quad (137)$$

(strongly dependent on the incoming gamma-ray energy distribution).

The constraint $X > 1$ corresponds to

$$\epsilon(2-\epsilon) < \frac{1}{\Theta M} \quad (138)$$

and is always fulfilled when $M\Theta < 1$. In the opposite case of $M\Theta > 1$, the constraint only allows electron energies between $1 \leqslant E \leqslant (1/4\Theta)$, in agreement with our initial assumption $4\Theta E\ln\tau_0 \ll 1$.

8.2. Electron Production Spectrum for $E \gg \tau_0\Theta^{-1}$

The first integral in Equation (122) can be approximated as

$$\begin{aligned} j_1 &= \int_{4\Theta E}^{2E} dz\, z^{q-(4+p)}[(z-1)^{p+1}+(z-1)^{p-1}]e^{-\frac{z}{4\Theta E}} \\ &\simeq \int_{4\Theta E}^{2E} dz\, z^{q-3}\left[1-\frac{p+1}{z}\right]e^{-\frac{z}{4\Theta E}} \end{aligned} \quad (139)$$

because in this energy range $z \geqslant 4\Theta E \gg 1$. We obtain

$$j_1 \simeq (4\Theta E)^{q-2}\frac{2c_1(q)}{q} \quad (140)$$

with the constant of order unity

$$c_1(q) = \frac{q}{2}e^{-1}U(1,q-1,1) = \frac{q\Gamma(q-2,1)}{2}, \quad (141)$$

which is tabulated in Table 1.

We find for the second integral in Equation (122) with the substitution $z = 1/w$

$$\begin{aligned} j_2(p) &= \int_{\frac{M}{M-E}}^{4\Theta E} dz\, z^{-(2+p)}[(z-1)^{p+1}+(z-1)^{p-1}] \\ &= \int_{\frac{1}{4\Theta E}}^{\frac{M-E}{M}} \frac{dw}{w}\left[(1-w)^{p+1}+w^2(1-w)^{p-1}\right]. \end{aligned} \quad (142)$$

Table 1
The Constant $c_1(q)$ for Different Values of q

q	$c_1(q)$
1.0	0.074
1.5	0.134
2.0	0.219
2.5	0.349
3.0	0.552
3.5	0.889
4.0	1.472

For integer values of $p = 1, 2, \ldots,$ the integral $j_2(p)$ can be solved exactly, e.g.,

$$j_2(1) = \ln\frac{1}{X} - \frac{1}{2\Theta E}\left(\frac{1}{X} - 1\right) + \frac{1}{(4\Theta E)^2}\left(\frac{1}{X^2} - 1\right). \quad (143)$$

For general values of p we use the expansion for $w < 1$

$$(1-w)^{p+1} + w^2(1-w)^{p-1} \simeq 1 - (p+1)w + \frac{p^2+p+2}{2}w^2, \quad (144)$$

yielding the approximation

$$j_2(p) \simeq \ln\frac{1}{X} - \frac{p+1}{4\Theta E}\left(\frac{1}{X} - 1\right) + \frac{p^2+p+2}{4\,(4\Theta E)^2}\left(\frac{1}{X^2} - 1\right), \quad (145)$$

which for $p = 1$ agrees exactly with Equation (143).

Collecting terms, we obtain for Equation (122)

$$T_1(E \gg \tau_0\Theta^{-1}) \simeq \frac{(4\Theta E)^q}{q} H[1-X] \times \left[\ln\frac{1}{X} + \frac{p+1}{4\Theta E}\left[1 - \frac{1}{X}\right] + c_1(q)\right], \quad (146)$$

or

$$T_1\left(\epsilon \gg \frac{2}{\Theta M}\right) \simeq \frac{(2\Theta M)^q}{q} H[1-X]\epsilon^q \times \left[\ln\frac{1}{X} + \frac{p+1}{2\Theta M\epsilon}\left[1 - \frac{1}{X}\right] + c_1(q)\right]. \quad (147)$$

The electron production spectrum (127) at high energies then becomes

$$\frac{dN}{d\epsilon}\left(\epsilon \gg \frac{2\tau_0}{\Theta M}\right) \simeq \frac{3\tau_0 I_0 H[1-X]}{\Gamma(q)\Theta M^p}\epsilon^{-(1+p)}S(\epsilon) \quad (148)$$

with the function

$$S(\epsilon) = \frac{2^{p-1}}{q}\left[c_1(q) + \ln\frac{1}{X} + \frac{p+1}{2\Theta M\epsilon}\left[1 - \frac{1}{X}\right]\right]. \quad (149)$$

The electron production spectrum at high energies is the product of the power law ($\propto \epsilon^{-(p+1)}$), reflecting the incoming gamma-ray energy spectrum, and the distribution $S(\epsilon)$.

The constraint $X < 1$ for $\Theta M \gg 1$ corresponds to electron energies between $1/(4\Theta) \leqslant E \leqslant M - (1/4\Theta)$, which agrees with our original assumption $4\Theta E \gg 1$.

8.3. Electron Production Spectra at Intermediate Energies $(1/\Theta \ln\tau_0) \leqslant E \leqslant \tau_0/\Theta$

The details of the approximations are given in Appendix D. We derive approximately

$$\frac{dN}{d\epsilon}(\epsilon, q=2) \simeq \frac{3\pi^{1/2} I_0 \Theta^{\frac{1}{2}} H[M-2]\epsilon^{-(p-\frac{1}{2})}}{2^{3-p} M^{p-\frac{3}{2}}}. \quad (150)$$

9. SUMMARY OF THE DERIVED ELECTRON PRODUCTION SPECTRA

Summarizing the main results of the last two sections, we notice that the approximations of the electron production spectrum depend on the value of the maximum gamma-ray energy M with respect to $M_c = \Theta^{-1}$, which is determined by the inverse soft photon temperature Θ^{-1}.

9.1. Maximum Gamma-ray Energies $2 \ll M \ll M_c$

In the case $2 \ll M \ll M_c$, only soft photons in the exponential tail of the Wien distribution overcome the threshold for pair production. As a result the maximum electron energy $E_{\max} \simeq M - (1/2)$ is well below $(\Theta \ln\tau_0)^{-1}$ and the electron production spectrum is given by Equations (134) and (136) providing

$$\frac{dN}{d\epsilon}\left(1 - \sqrt{1 - \frac{2}{M}} \leqslant \epsilon \leqslant 1 + \sqrt{1 - \frac{2}{M}}, \Theta M \ll 1\right) \simeq A_0(\Theta M)^{3-q}\epsilon^{1-q}(2-\epsilon)^{3-q}[1 + (1-\epsilon)^2]e^{-\frac{1}{\Theta M\epsilon(2-\epsilon)}}, \quad (151)$$

with the abbreviation

$$A_0 = \frac{3\tau_0 I_0}{4\Gamma(q)\Theta M^p}. \quad (152)$$

Due to the dominating exponential function

$$e^{-\frac{1}{\Theta M\epsilon(2-\epsilon)}} \leqslant e^{-(\Theta M)^{-1}} = e^{-(M_c/M)} \ll 1, \quad (153)$$

the pair production spectrum in this case is strongly peaked at $\epsilon = 1$. This corresponds to half of the maximum gamma-ray energy ($E = M/2$), though it is strongly exponentially reduced (see Figure 6), as indicated by the extremely small numbers at the vertical scale.

9.2. Ultrahigh Maximum Gamma-ray Energies $M \gg M_c$

In the opposite case $M \gg M_c$ most of the low-energy soft photons from the power-law part of the Wien distribution also overcome the threshold for pair production. Here the electron production spectrum is more involved; it is given by the still exponentially reduced Equations (134) and (137) at electron energies $E \leqslant (\Theta \ln\tau_0)^{-1}$, Equation (150) at electron energies $E \in [(\Theta \ln\tau_0)^{-1}, \tau_0/\Theta]$, and Equation (148) at electron energies $(\tau_0/\Theta) \leqslant E \leqslant M - (1/2)$.

As a rough analytical expression, to reproduce all essential features of these three different approximations, we use in the case of $q = 2$, for which we derived approximation (150),

$$\frac{dN}{d\epsilon}\left(1 - \sqrt{1 - \frac{2}{M}} \leqslant \epsilon \leqslant 1 + \sqrt{1 - \frac{2}{M}}, \Theta M \gg 1\right) \simeq A_1 e^{-\frac{2}{\Theta M\epsilon\ln\tau_0}} \frac{\epsilon^{\frac{1}{2}-p}}{1 + \frac{\pi^{1/2}}{2\tau_0 c_1(2)}(\Theta M\epsilon)^{3/2}} = A_1 e^{-\frac{2}{\Theta M\epsilon\ln\tau_0}} \frac{\epsilon^{\frac{1}{2}-p}}{1 + \frac{4}{\tau_0}(\Theta M\epsilon)^{3/2}}, \quad (154)$$

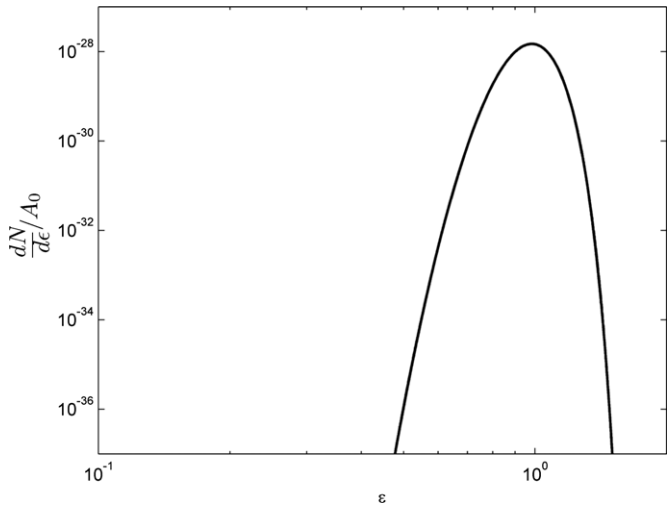

Figure 6. Approximation (151) of the energy spectrum of generated pairs $N(\epsilon)/A_0$ from a power-law-distributed gamma-ray beam $\propto k_1^{-3} H[M - k_1]$ below the maximum gamma-ray energy $M = 10^5$ interacting with isotropically distributed soft photons with a Wien distribution with spectral index $q = 2$ and temperature $\Theta = 1.6 \times 10^{-7}$ (corresponding to 0.08 eV), so that $M_c = 1/\Theta = 6 \times 10^6$. Because M is a factor of 60 smaller than M_c in this example, only soft photons in the exponential tail of the Wien distribution overcome the threshold for pair production, so that the generated pair production spectrum is exponentially reduced (see the small numbers at the vertical axis).

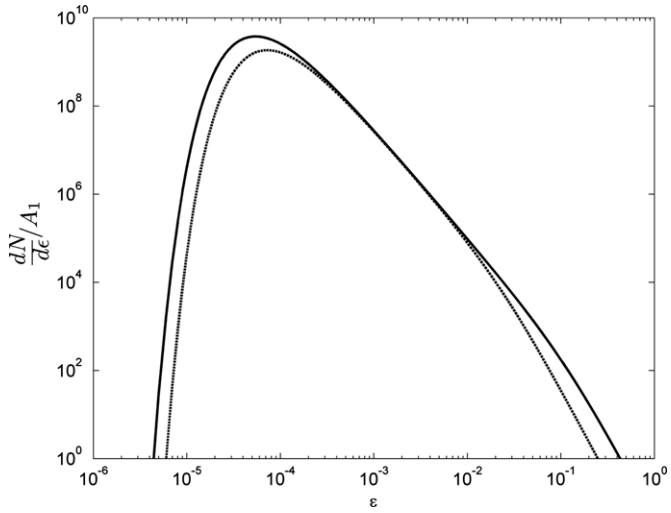

Figure 7. Approximation (154) of the energy spectrum of generated pairs $N(\epsilon)/A_1$ from a power-law-distributed gamma-ray beam $\propto k_1^{-3} H[M - k_1]$ for the maximum gamma-ray energy $M = 10^{10}$ interacting with isotropically distributed soft photons with a Wien distribution with spectral index $q = 2$ and temperature $\Theta = 1.6 \times 10^{-7}$ (corresponding to 0.08 eV), so that $M_c = 1/\Theta = 6 \times 10^6$. Two different values of the optical depth, $\tau_0 = 10^3$ (dotted line) and $\tau_0 = 10^4$ (full line), are adopted. Note that at intermediate electron energies $\epsilon \in [\epsilon_1, \epsilon_2] = 1.2 \times 10^{-3} [(\ln \tau_0)^{-1}, \tau_0]$ the production spectrum is independent of the actual value of τ_0.

with the abbreviation

$$A_1 = \frac{3\pi^{1/2} I_0 \Theta^{\frac{1}{2}}}{2^{3-p} M^{p-\frac{3}{2}}}. \quad (155)$$

This spectrum is shown in Figure 7 for the two values of $\tau_0 = 10^3$ and $\tau_0 = 10^4$. In both cases the low-energy part below $\epsilon < \epsilon_1 = (2M_c/M \ln \tau_0)$ exhibits a strong exponential cutoff, whereas the spectrum at very high energies $\epsilon > \epsilon_1 = 2M_c\tau_0/M$ exhibits the steep power law $\propto \epsilon^{-1-p}$. At intermediate energies the production spectrum is independent of the actual value of

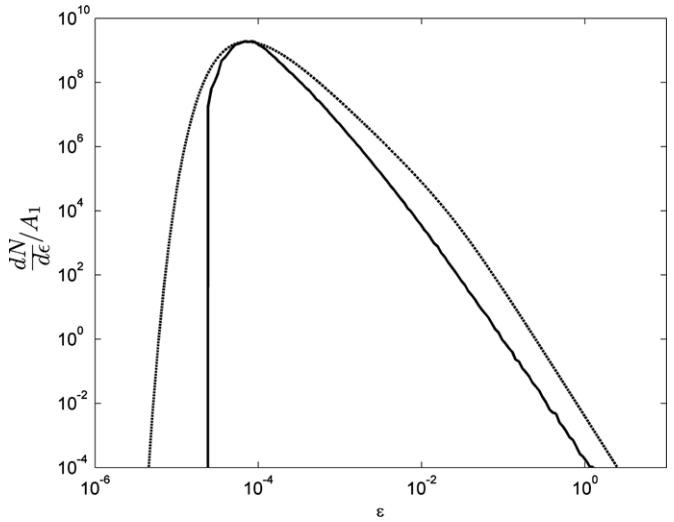

Figure 8. Comparison of the analytically calculated (dotted line) with the numerically calculated (full line) production spectrum of generated pairs from a power-law-distributed gamma-ray beam $\propto k_1^{-3} H[M - k_1]$ for the maximum gamma-ray energy $M = 10^{10}$ interacting with isotropically distributed soft photons with a Wien distribution with spectral index $q = 2$ and temperature $\Theta = 1.6 \times 10^{-7}$ (corresponding to 0.08 eV). An optical depth of $\tau_0 = 10^3$ is adopted.

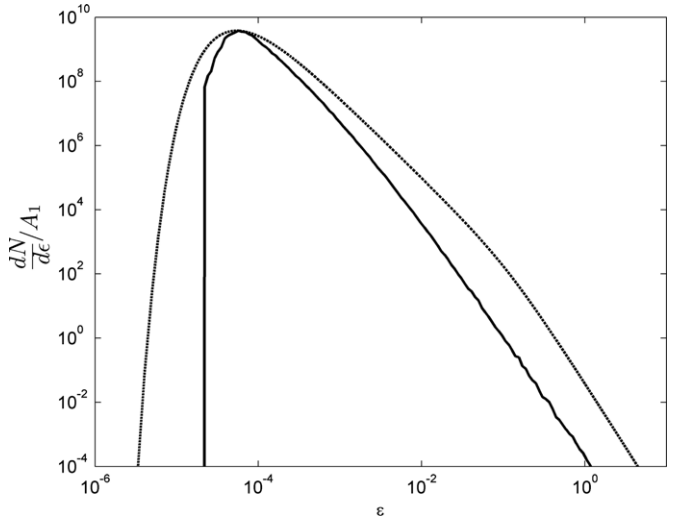

Figure 9. Same as Figure 8 for an adopted optical depth of $\tau_0 = 10^4$.

τ_0, as discussed in Section 7.2. However, the extension of the energy spectrum depends on the value of τ_0 as $\epsilon_1 \propto (\ln \tau_0)^{-1}$ and $\epsilon_2 \propto \tau_0$ become smaller and larger with increasing τ_0, respectively. The energy spectrum peaks near ϵ_1, corresponding to $E_1 = M\epsilon_1/2 = M_c/\ln \tau_0$ for gamma-ray spectral indices $p > 0.5$, and at ϵ_2, corresponding to $E_2 = M\epsilon_2/2 = M_c\tau_0$ for $p < 0.5$. In Figures 8 and 9, we compare our analytical production spectrum (from Figure 7) with the numerically calculated production spectrum using the code of Elyiv et al. (2009) for optical depths $\tau_0 = 10^3$ (Figure 8) and $\tau_0 = 10^4$ (Figure 9), respectively. In this simulation we do not include the effects of the extragalactic magnetic field as well as the IC interactions with CMB photons, instead calculating only the generated pair energy distribution resulting from the first double photon collisions. The analytical and numerical curves have been normalized at the maximum of the production spectrum. Apart from very low gamma-ray energies, the level of agreement is remarkably high: the spectral form and the

location of the maximum are identical. These agreements justify a posteriori the assumptions that allowed our analytic approximation.

10. SUMMARY AND CONCLUSIONS

The detection of about 30 blazars at cosmological distances with strong TeV photon emission has renewed interest in the production of relativistic pairs in double photon collisions of the beamed gamma rays with the isotropically distributed EBL in the IGM. The generated pair beams can probe cosmological magnetic fields in cosmic voids; their deposited energy might also affect the thermal history of the IGM.

The typical energies $k_0 \simeq 10^{-7}$ in units of $m_e c^2$ of the EBL are more than 10 orders of magnitude smaller than the observed gamma-ray energies $k_1 \geqslant 10^7$. Using the limit $k_0 \ll k_1$, we demonstrated from the relativistic kinematics that the angular distribution of the generated pairs from the double photon collision processes in the lab frame is highly beamed in the direction of the initial gamma-ray photons, an obvious expected result but one proven explicitly here.

We also analytically calculated anew the energy spectrum (Equation (63)) of the generated pairs from a monoenergetic beamed gamma ray interacting with a monoenergetic, gyrotropically and isotropically distributed soft photon distribution. Despite its different analytical form, it agrees perfectly with the earlier derived production spectrum of Aharonian et al. (1983) and with the numerically computed energy spectrum based on the work of Elyiv et al. (2009). The analytic energy spectrum (63) serves as a kernel to derive analytically by two integrations the electron energy production spectrum (101) for arbitrary gamma-ray energy distributions and arbitrary soft photon energy distributions.

As blazar observations often indicate power-law distributions of the emitted gamma-ray beam with $I(k_1) = I_0 k^{-p}$ for $k_1 \leqslant M$, we studied this case in more detail, adopting a Wien-type $N(k_0) \propto k_0^q \exp(-k_0/\Theta)$ soft photon energy distribution, which represents both graybody distributed target photons and flat ($q > -1$) power-law target photons with an exponential cutoff. For the astrophysically important case of the Wien distribution with $q > 1$, the two integrals of the production spectrum (101) can be evaluated approximately in closed form—providing the analytical approximations for the electron production spectrum. For distant objects with luminosity distances $d_L \gg r_0 = 0.49 N_0^{-1}$ Mpc, the implied large values of the optical depth $\tau_0 = d_L/r_0$ indicate that the electron production spectra differ at energies E inside and outside the interval $[(\Theta \ln \tau_0)^{-1}, \tau_0/\Theta]$, provided the maximum gamma-ray energy $M \gg \Theta^{-1}$. Outside this interval the electron production takes place in the optically thin limit with respect to pair production, whereas inside this interval the electron production becomes independent of τ_0, as any gamma-ray photon can only generate two electrons. For maximum gamma-ray energies $M \ll \Theta^{-1}$ this optically thick behavior does not occur. Here the pair production spectrum is strongly peaked at half of the maximum gamma-ray energy ($E = M/2$), but also strongly exponentially reduced, as only soft photons in the exponential tail of the Wien distribution overcome the threshold for pair production.

In the opposite case $M \gg \Theta^{-1}$ low-energy soft photons from the power-law part of the Wien distribution also participate in the pair production process. Here the production spectrum is strongly peaked near $E \simeq \Theta^{-1}$, the inverse of the soft photon temperature, which is exponentially reduced at small energies and decreasing with the steep power law $\propto E^{-1-p}$ up to the maximum energy $E = M - (1/2)$.

We are grateful to the referee for a very constructive report on a difficult manuscript. R.S. and D.I. gratefully acknowledge partial support of this work by the German Ministry for Education and Research (BMBF) through Verbundforschung Astroteilchenphysik grant 05A11PCA and the Deutsche Forschungsgemeinschaft through grant Schl 201/23-1. A.E. is the beneficiary of a fellowship granted by the Belgian Federal Science Policy Office.

APPENDIX A

THE INTEGRAL (49)

With $B = 1 - A^2$ the integral (47) reads

$$I(E, k_1, k_0) = (1 - B) I_0 + I_1 + \frac{8}{k_1^2} I_2 - \frac{32}{k_1^4} I_3 - \frac{32(1 - B)}{k_1^4} I_4, \tag{A1}$$

with

$$I_0 = \int_{x_2(T)}^{4k_0/k_1} dx \, \frac{1}{\sqrt{1 - x}(B - x)}, \tag{A2}$$

$$I_1 = \int_{x_2(T)}^{4k_0/k_1} dx \, \frac{\sqrt{1 - x}}{B - x}, \tag{A3}$$

$$I_2 = \int_{x_2(T)}^{4k_0/k_1} dx \, \frac{\sqrt{1 - x}}{x(B - x)}, \tag{A4}$$

$$I_3 = \int_{x_2(T)}^{4k_0/k_1} dx \, \frac{\sqrt{1 - x}}{x^2(B - x)}, \tag{A5}$$

and

$$I_4 = \int_{x_2(T)}^{4k_0/k_1} dx \, \frac{\sqrt{1 - x}}{x^2(B - x)^2} = -\frac{\partial I_3}{\partial B}. \tag{A6}$$

Using

$$\frac{1}{x(B - x)} = \frac{1}{B}\left[\frac{1}{x} + \frac{1}{B - x}\right]$$

provides

$$B I_2 = I_1 + I_5,$$
$$I_5 = \int_{x_2(T)}^{4k_0/k_1} dx \, \frac{\sqrt{1 - x}}{x} = -I_1(B = 0), \tag{A7}$$

so that

$$I(E, k_1, k_0) = (1 - B) I_0 + \left(1 + \frac{8}{B k_1^2}\right) I_1 + \frac{8 I_5}{B k_1^2} + \frac{32}{k_1^4}\left[(1 - B)\frac{\partial I_3}{\partial B} - I_3\right]. \tag{A8}$$

For I_3 we write Equation (A7)

$$I_3 = \frac{1}{B}\int_{x_2(T)}^{4k_0/k_1} dx \, \frac{\sqrt{1 - x}}{x^2(B - x)}(B - x + x)$$
$$= \frac{1}{B}[I_6 + I_2] = \frac{I_6}{B} + \frac{1}{B^2}[I_1 + I_5] \tag{A9}$$

with

$$I_6 = \int_{x_2(T)}^{4k_0/k_1} dx\,\frac{\sqrt{1-x}}{x^2} = -I_2(B=0). \tag{A10}$$

The remaining anti-derivatives are (Gradshteyn & Ryzhik 1980)

$$I_0(B) = \frac{1}{(1-B)^{1/2}}\ln\frac{(1-B)^{1/2}+(1-x)^{1/2}}{(1-B)^{1/2}-(1-x)^{1/2}} = \frac{2}{(1-B)^{1/2}}\mathrm{artanh}\left(\frac{1-x}{1-B}\right)^{1/2} \tag{A11}$$

and

$$I_1(B) = (1-B)^{1/2}\ln\frac{(1-B)^{1/2}+(1-x)^{1/2}}{(1-B)^{1/2}-(1-x)^{1/2}} - 2(1-x)^{1/2} = 2(1-B)^{1/2}\,\mathrm{artanh}\left(\frac{1-x}{1-B}\right)^{1/2} - 2(1-x)^{1/2}, \tag{A12}$$

so that

$$I_5 = -I_1(B=0) = 2(1-x)^{1/2} - \ln\frac{1+(1-x)^{1/2}}{1-(1-x)^{1/2}} = 2(1-x)^{1/2} - 2\mathrm{artanh}\,(1-x)^{1/2}. \tag{A13}$$

Likewise,

$$I_6 = \frac{1}{2}\ln\frac{1+(1-x)^{1/2}}{1-(1-x)^{1/2}} - \frac{(1-x)^{1/2}}{x} = \mathrm{artanh}\,(1-x)^{1/2} - \frac{(1-x)^{1/2}}{x}. \tag{A14}$$

For Equation (A9) we obtain

$$I_3(B) = \frac{2(1-B)^{1/2}}{B^2}\mathrm{artanh}\left(\frac{1-x}{1-B}\right)^{1/2} - \frac{2-B}{B^2}\mathrm{artanh}\,(1-x)^{1/2} - \frac{(1-x)^{1/2}}{Bx}, \tag{A15}$$

so that

$$\frac{\partial I_3}{\partial B} = \frac{(B-2x)(1-x)^{1/2}}{B^2x(B-x)} + \frac{4-B}{B^3}\mathrm{artanh}\,(1-x)^{1/2} + \frac{3B-4}{(1-B)^{1/2}B^3}\mathrm{artanh}\left(\frac{1-x}{1-B}\right)^{1/2}. \tag{A16}$$

This provides for

$$(1-B)\frac{\partial I_3}{\partial B} - I_3(B) = \frac{[B+(B-2)x](1-x)^{1/2}}{B^2x(B-x)} + \frac{4-3B}{B^3} \times\left[\mathrm{artanh}\,(1-x)^{1/2} - \frac{(4-B)(1-B)^{1/2}}{B^3}\mathrm{artanh} \times\left(\frac{1-x}{1-B}\right)^{1/2}\right]. \tag{A17}$$

The integral (A8) finally becomes

$$I(E,k_1,k_0) = R[4k_0/k_1] - R[x_2(T)], \tag{A18}$$

with

$$R[x] = 4(1-B)^{1/2}\left[1+\frac{4}{Bk_1^2} - \frac{8(4-B)}{B^3k_1^4}\right]\mathrm{artanh}\left(\frac{1-x}{1-B}\right)^{1/2} + \frac{16}{Bk_1^2}\left[\frac{2(4-3B)}{B^2k_1^2} - 1\right]\mathrm{artanh}\,(1-x)^{1/2} + 2\left[\frac{16[B+(B-2)x]}{B^2k_1^4x(B-x)} - 1\right](1-x)^{1/2}. \tag{A19}$$

With $B = 1 - A^2$, Equation (50) is obtained.

APPENDIX B

THE INTEGRAL (79)

The integral (79) reads

$$I_7(m) = \int_0^m dy\,\frac{\ln(1-y)+\ln(1+y)}{(1-y)(1+y)} = \frac{1}{2}\left[\int_0^m dy\,\frac{\ln(1+y)}{1+y} + \int_0^m dy\,\frac{\ln(1-y)}{1-y} + \int_0^m dy\,\frac{\ln(1+y)}{1-y} + \int_0^m dy\,\frac{\ln(1-y)}{1+y}\right]. \tag{B1}$$

The first two integrals can be directly solved. Partially integrating the forth integral we find

$$I_7(m) = \frac{1}{4}[\ln^2(1+m) - \ln^2(1-m)] + \frac{1}{2}\ln(1-m)\ln(1+m) - I_8(m) \tag{B2}$$

with

$$I_8(m) = \int_0^m dy\,\frac{\ln(1+y)}{y-1} = \int_1^{1+m} dx\,\frac{\ln(x+2)}{x}. \tag{B3}$$

Substituting $x = 2s$ yields

$$I_8(m) = \ln 2\int_1^{1+m}\frac{dx}{x} + \int_{\frac{1}{2}}^{\frac{1+m}{2}} dx\,\frac{\ln(s+1)}{s} = \ln 2\ln(1+m) + \mathrm{Li}\left[\frac{1}{2},\frac{1+m}{2}\right]. \tag{B4}$$

Collecting terms in Equation (B2) then provides the result (79).

APPENDIX C

APPROXIMATIVE EVALUATION OF THE INTEGRAL (109)

All y-integrals not involving the $\ln(1+y)$-function can be expressed as the difference of two incomplete gamma functions. However, for small nonrelativistic value of the dimensionless soft photon temperature $\Theta \ll 1$, we evaluate the integral (111) here approximately. For values of

$$\frac{4\Theta E}{z} \geqslant \frac{2E}{z} - 1,$$

corresponding to

$$z \geqslant 2E(1-2\Theta) \simeq 2E, \tag{C1}$$

the exponential functions in the integral (109) can be well approximated by unity. However, this case is of no relevance here because z is limited in the integrals (114) and (115) to $2E$. The opposite case

$$z \leqslant 2E(1-2\Theta) \simeq 2E \tag{C2}$$

holds over the whole range of z-values, and allows us to approximate the exponential functions in the integral (109) by unity for $y \leqslant \alpha = 4\Theta E/z$ and for zero otherwise. Consequently, we obtain

$$\begin{aligned} J(E,\Theta,z) &\simeq J(\alpha) \\ &= 4\int_0^\alpha dy\,(1+y)^{q-3}[(1+y)\ln(1+y)-y] \\ &\quad + \frac{z^2-2z+2}{z-1}\int_0^\alpha dy\,y(1+y)^{q-2} \end{aligned} \tag{C3}$$

with

$$\alpha = \frac{4\Theta E}{z}. \tag{C4}$$

After straightforward, but tedious, integrations we derive

$$\begin{aligned} J(\alpha) &= 4(1+\alpha)^{q-2}\left[\frac{(1+\alpha)\ln(1+\alpha)}{q-1} - \frac{\alpha}{q-2}\right] \\ &\quad + \frac{4}{(q-2)(q-1)^2}[(1+\alpha)^{q-1}-1] \\ &\quad + \frac{z^2-2z+2}{(q-1)(z-1)}\left[\alpha(1+\alpha)^{q-1} - \frac{(1+\alpha)^q-1}{q}\right] \end{aligned} \tag{C5}$$

with the asymptotics

$$J(\alpha) \simeq \left[z-1+\frac{1}{z-1}\right]\begin{cases} \frac{\alpha^2}{2} & \text{for } \alpha \leqslant 1 \\ \frac{\alpha^q}{q} & \text{for } \alpha > 1. \end{cases} \tag{C6}$$

APPENDIX D

ELECTRON PRODUCTION SPECTRA AT INTERMEDIATE ENERGIES $(1/\Theta \ln\tau_0) \leqslant E \leqslant \tau_0/\Theta$

Here the electron production spectrum (114) reads

$$\frac{dN}{d\epsilon}(\epsilon) = \frac{3I_0H[M-2]e^{\frac{2}{M\Theta\epsilon}}}{2^{q+2-p}\Gamma(q)\Theta^q M^{p+q-1}\epsilon^{q+p}}T_2(\epsilon), \tag{D1}$$

with the integral

$$T_2(\epsilon) = \int_{\frac{2}{2-\epsilon}}^{M\epsilon} dz\,z^{q-p}(z-1)^{p-1}e^{-\frac{(z+\frac{4}{z})}{4\Theta E}}J\left(\frac{2\Theta M\epsilon}{z}\right). \tag{D2}$$

We restrict the analysis to the Wien power-law spectral index $q=2$, so that the asymptotics (116)

$$J(\alpha) = \left[z-1+\frac{1}{z-1}\right]\frac{\alpha^2}{2} \tag{D3}$$

hold for all values of α. We find

$$\begin{aligned} T_2(\epsilon, q=2) &= 2(\Theta M)^2\epsilon^2 \\ &\quad \times \int_{\frac{2}{2-\epsilon}}^{M\epsilon} dz\,z^{-p}[(z-1)^p + (z-1)^{p-2}]e^{-\frac{(z+\frac{4}{z})}{2\Theta M\epsilon}}, \end{aligned} \tag{D4}$$

so that

$$\frac{dN}{d\epsilon}(\epsilon, q=2) = \frac{3I_0H[M-2]\epsilon^{-p}e^{\frac{2}{M\Theta\epsilon}}}{2^{3-p}M^{p-1}}T_3(\epsilon) \tag{D5}$$

with the integral

$$\begin{aligned} T_3(\epsilon) &= \int_{\frac{2}{2-\epsilon}}^{M\epsilon} dz\,z^{-p}[(z-1)^p + (z-1)^{p-2}]e^{-\frac{(z+\frac{4}{z})}{2\Theta M\epsilon}} \\ &\simeq \int_{\frac{2}{2-\epsilon}}^{M\epsilon} dz\left[1-\frac{p}{z}\right]e^{-\frac{(z+\frac{4}{z})}{2\Theta M\epsilon}} = \int_{\frac{2}{2-\epsilon}}^{M\epsilon} dz\,\exp[-F(z)], \end{aligned} \tag{D6}$$

where

$$F(z) = \frac{z+\frac{4}{z}}{2\Theta M\epsilon} = w\left[\frac{1}{z}+\frac{z}{4}\right] \tag{D7}$$

with

$$w = \frac{2}{\Theta M\epsilon}. \tag{D8}$$

In the approximation (D6) we used $z \geqslant 2$. The remaining integral (D6) is solved by the method of steepest descent.

The function $F(z)$ attains its minimum value $F(z_0) = w$ at $z_0 = 2$. With the approximation

$$F(z) \simeq F(z_0) + \frac{1}{2}F''(z_0)(z-z_0)^2 = w + \frac{w}{8}(z-2)^2 \tag{D9}$$

inserted, we obtain for the integral (D6)

$$\begin{aligned} T_3(w) &\simeq \sqrt{\frac{2\pi}{w}}e^{-w}\left(\mathrm{erf}\left[\sqrt{\frac{w}{8}}(M\epsilon-2)\right]\right. \\ &\quad \left. + \mathrm{erf}\left[\sqrt{\frac{w}{2}}\frac{1-\epsilon}{2-\epsilon}\right]\right) \end{aligned} \tag{D10}$$

in terms of the error function. We find for the electron production spectrum (D5)

$$\epsilon^{p-\frac{1}{2}}\frac{dN}{d\epsilon}(\epsilon, q=2) = \frac{3\pi^{1/2}I_0\Theta^{\frac{1}{2}}H[M-2]}{2^{3-p}M^{p-\frac{3}{2}}}T_4(w) \tag{D11}$$

with the function

$$\begin{aligned} T_4(w) &= \mathrm{erf}\left[\sqrt{\frac{w}{2}}\left(\frac{M\epsilon}{2}-1\right)\right] + \mathrm{erf}\left[\sqrt{\frac{w}{2}}\frac{1-\epsilon}{2-\epsilon}\right] \\ &= \mathrm{erf}\left[\frac{1-\Theta w}{\sqrt{2w\Theta}}\right] + \mathrm{erf}\left[\sqrt{\frac{w}{2}}\frac{1-\frac{2}{\Theta M w}}{2-\frac{1}{\Theta M w}}\right]. \end{aligned} \tag{D12}$$

In this electron energy range the function w varies between $w \in [1/\ln\tau_0, \tau_0]$. Given the extreme smallness of $\Theta \ll 1$; the argument of the first error function in Equation (D12) is large compared to unity. This allows us to approximate $T_4(w) \simeq 1$, as the argument of the second error function is a factor $\Theta w/2$ smaller than the argument of the first error function. We then obtain for the electron production spectrum (D11) at intermediate energies

$$\frac{dN}{d\epsilon}(\epsilon, q=2) \simeq \frac{3\pi^{1/2}I_0\Theta^{\frac{1}{2}}H[M-2]\epsilon^{-(p-\frac{1}{2})}}{2^{3-p}M^{p-\frac{3}{2}}}. \tag{D13}$$

REFERENCES

Abramowitz, M., & Stegun, I. A. 1972, Handbook of Mathematical Functions (Washington, DC: NBS)

Abramowski, A., Acero, F., Aharonian, F., et al. (HESS Collaboration), 2012, A&A, 538, A103

Aharonian, F. A. 2003, Very High Energy Cosmic Gamma Radiation (Singapore: World Scientific), Equations (3–25)

Aharonian, F. A., Akhperjanian, A. G., Bazer-Bachi, A. R., et al. (HESS Collaboration), 2006, Nature, 440, 1018

Aharonian, F. A., Atoyan, A. M., & Nagapetian, A. M. 1983, Astrofizika (Astrophysics), 19, 187

Aharonian, F. A., Coppi, P. S., & Völk, H. J. 1994, ApJ, 423, L5

Bonometto, S., & Rees, M. J. 1971, MNRAS, 152, 21

Böttcher, M., & Schlickeiser, R. 1997, A&A, 325, 866

Broderick, A. E., Chang, P., & Pfrommer, C. 2012, ApJ, 732, 22

Cerutti, B., Dubus, G., & Henri, G. 2009, A&A, 507, 1217

Elyiv, A., Neronov, A., & Semikoz, D. V. 2009, Phys. Rev. D, 80, 023010

Franceschini, A., Rodighiero, G., & Vaccari, M. 2008, A&A, 487, 837

Gould, R. J., & Schreder, G. P. 1967, Phys. Rev., 155, 1404

Gradshteyn, I. S., & Ryzhik, I. M. 1980, Tables of Integrals, Series and Products (New York: Academic)

Hagedorn, R. 1973, Relativistic Kinematics (Reading, MA: Benjamin)

Hinton, J. A., & Hofmann, W. 2009, ARA&A, 47, 523

Jauch, J. M., & Rohrlich, F. 1955, Theory of Photons and Electrons (Reading, MA: Addison-Wesley)

Kneiske, T. M., Bretz, T., Mannheim, K., & Hartmann, D. H. 2004, A&A, 413, 807

Neronov, A., & Semikoz, D. 2009, Phys. Rev. D, 80, 123012

Neronov, A., & Vovk, I. 2010, Science, 328, 73

Schlickeiser, R., Ibscher, D., & Supsar, M. 2012, ApJ, 758, 102